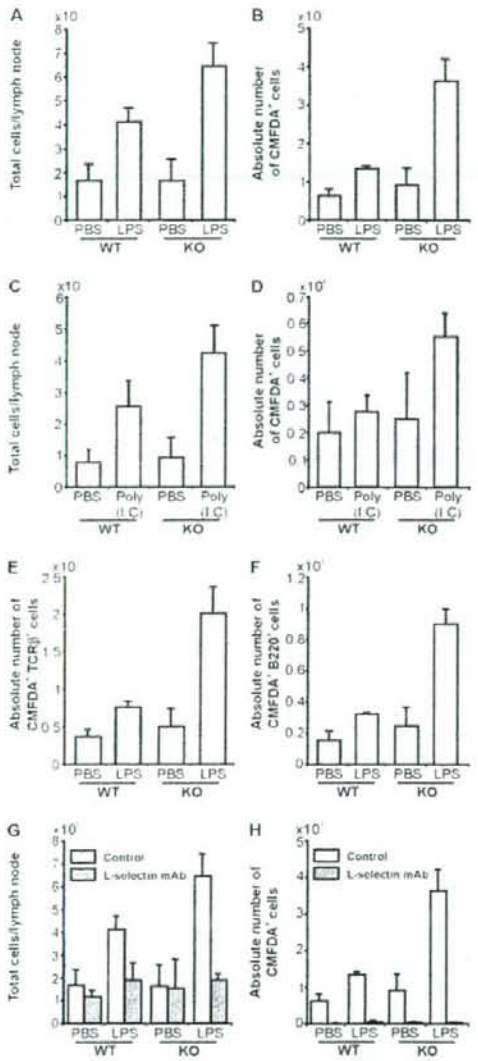

FIGURE 2. *Cd73*-deficient mice have large draining lymph nodes and high rates of L-selectin-dependent lymphocyte migration after an inflammatory stimulus. LPS (1 μg; *A*, *B*, *E*, *F*, *G*, and *H*) or poly(I:C) (5 μg; *C* and *D*) was injected into the left front footpad (or thigh; *C* and *D*) of $cd73^{+/+}$ and $cd73^{-/-}$ mice, and an equivalent volume of PBS was injected into the right front footpad (or thigh; *C* and *D*). Twenty-four hours later, the mice were injected with 10^7 CMFDA-labeled $cd73^{+/+}$ splenocytes i.v. One hour later, brachial (or inguinal; *C* and *D*) lymph nodes were harvested, and the total numbers of cells in each lymph node were counted. *A* and *C*, The lymph node cells were then stained with PE anti-TCRβ and allophycocyanin anti-B220 (CD45R). The percentages of fluorescent cells were determined by flow cytometry, and the absolute numbers of total lymphocytes (*B* and *D*), T cells (*E*), and B cells (*F*) that migrated to the lymph nodes in 1 h were calculated. In some experiments, the mice also received 50 μg of anti-L-selectin Ab MEL-14 i.v. at the same time as LPS/PBS. Twenty-four hours later, the mice were injected with 10^7 CMFDA-labeled $cd73^{+/+}$ splenocytes i.v. One hour later, lymph nodes were harvested and the total numbers of cells in each lymph node were counted (*G*). The percentages of $CMFDA^+$ cells were determined by flow cytometry, and the absolute numbers of total lymphocytes that migrated to the lymph nodes in 1 h were calculated (*H*). Data from mice not receiving anti-L-selectin Ab in *G* and *H* are the same as in *A* and *B*.

wild-type mice. These results suggest that it is CD73 on HEV (rather than on lymphocytes) that is responsible for the larger sizes of draining lymph nodes in *cd73*-deficient mice. Similar results were seen when poly(I:C), a TLR3 ligand, was used instead of LPS as the inflammatory stimulus (Fig. 2, *C* and *D*). Furthermore, staining with TCRβ (Fig. 2*E*) and B220 (Fig. 2*F*) Abs revealed that migration of both T and B lymphocytes was increased in *cd73*-deficient draining lymph nodes. Similar results were observed when LPS or poly(I:C) was injected into the rear footpad or thigh, as revealed by examination of popliteal or inguinal lymph nodes, respectively (our unpublished data).

Next, we asked whether the increased lymphocyte migration and enlarged lymph nodes seen in *cd73*-deficient mice were the result of increased migration across HEV. To address this question, mice were pretreated with L-selectin Ab. This Ab was chosen because lymphocyte-expressed L-selectin is known to initiate rolling on HEV (through its interaction with PNAd) and because administration of L-selectin Ab has been shown to diminish lymphocyte migration to peripheral lymph nodes under steady-state conditions in vivo (3, 42). We observed that treatment of mice with L-selectin Ab i.v. at the same time as LPS abrogated CMFDA-labeled lymphocyte migration even after 24 h in both strains of mice (Fig. 2*H*) and abolished the hallmark increased size of *cd73*-deficient draining lymph nodes (Fig. 2*G*).

Contribution of lymphocyte CD73 expression to migration across HEV

Because lymphocyte CD73 has been reported to be a signaling molecule, an adhesion molecule, and a maturation and subpopulation marker (16, 39), we next evaluated its role in lymphocyte migration into draining lymph nodes. We first examined the percentage of $CD4^+$, $CD8^+$, and $CD19^+$ lymphocytes that coexpressed CD73 in wild-type draining lymph nodes by flow cytometry 24 h after stimulation. LPS-induced lymph node hypertrophy did not affect the CD73 expression pattern compared with that in lymph nodes from the PBS-treated side (Fig. 3*A*). The CD73 expression pattern was also equivalent to that in naive lymph nodes and spleen (our unpublished data). We next evaluated migration of *cd73*-deficient lymphocytes compared with wild-type lymphocytes in both wild-type and *cd73*-deficient mice. This was done by injecting mice with a 1:1 mixture of splenocytes from $cd73^{+/+}$ and $cd73^{-/-}$ mice labeled with either CMFDA or CMTMR. Virtually identical ratios of $cd73^{-/-}$:$cd73^{+/+}$ lymphocytes were observed in both wild-type and *cd73*-deficient draining lymph nodes (Fig. 3*B*). These results suggest no bias between CD73-positive and -negative lymphocytes in their ability to migrate after an inflammatory stimulus. They further suggest that it is a lack of CD73 expression on HEV that is responsible for the increased migration of lymphocytes into draining lymph nodes of *cd73*-deficient mice.

Contribution of DC to increased draining lymph node size in $cd73^{-/-}$ mice

The accumulation of activated DC in draining lymph nodes is critical for the regulation of proinflammatory cytokine production and induction of vascular growth (15). Local injection of LPS is known

All results are expressed as mean ± SD and are representative of 3–10 experiments ($n = 4$–5 mice of each genotype for each experiment, $p < 0.025$ for all comparisons of wild type (WT) vs knockout (KO) in draining lymph nodes in *A*–*F*, for control vs MEL-14 in draining lymph nodes for *G*, and for control vs MEL-14 in all groups in *H*).

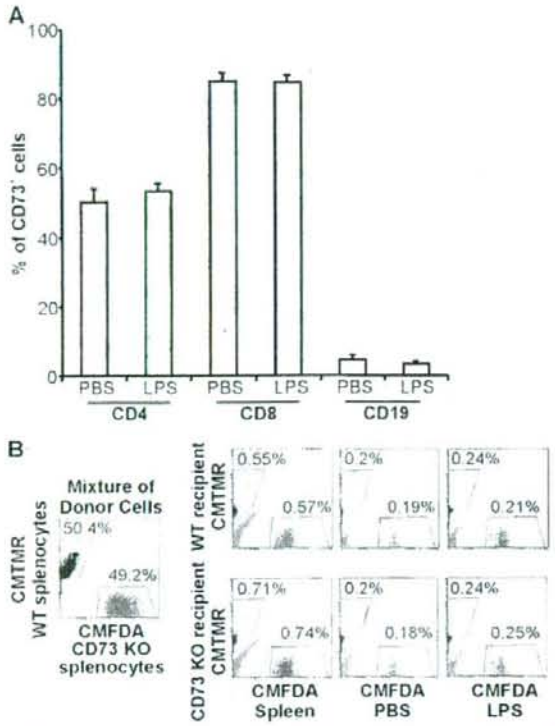

FIGURE 3. CD73-positive and -negative lymphocytes migrate equally well into inflamed lymph nodes. LPS (1 μg) was injected into the left rear footpad of $cd73^{+/+}$ mice, and an equivalent volume of PBS was injected into the right rear footpad. *A*, Twenty-four hours later, the popliteal lymph node cells were stained with FITC anti-CD4, FITC anti-CD8, or PE Cy5.5 anti-CD19 plus biotinylated anti-CD73 (TY/23) and PE-streptavidin or the relevant isotype-matched control Abs, and the percentages of $CD4^+$, $CD8^+$, and $CD19^+$ lymphocytes that coexpressed CD73 were determined by flow cytometry ($n = 4$ in each of two independent experiments). *B*, LPS (1 μg) was injected into the left thigh of $cd73^{-/-}$ and $cd73^{+/+}$ mice, and an equivalent volume of PBS was injected into the right thigh. Twenty-four hours later, the mice were injected i.v. with an equal mixture of 1×10^7 $cd73^{+/+}$ and $cd73^{-/-}$ splenocytes labeled with CMFDA or CMTMR, respectively. One hour later, inguinal lymph nodes were harvested, and the percentages of CMFDA$^+$ and CMTMR$^+$ lymphocytes were determined. Representative data from one of two experiments are shown.

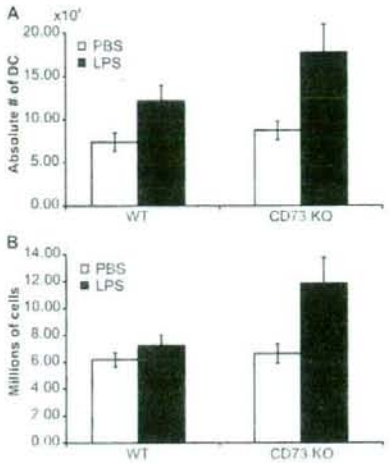

FIGURE 4. Migration of DC into draining lymph nodes after an inflammatory stimulus. LPS (1 μg) was injected into the left front footpad of $cd73^{+/+}$ and $cd73^{-/-}$ mice, and an equivalent volume of PBS was injected into the right front footpad. Six hours later, lymph nodes were digested with collagenase, DNase I, and trypsin, as described in *Materials and Methods*, and cells were counted and stained with FITC anti-MHC class II and PE anti-CD11c. Dead cells were excluded by propidium iodide staining. The average (±SEM) absolute numbers of MHC class II^{high} $CD11c^+$ cells are shown (*A*) as well as the total number of leukocytes/lymph node (*B*). The results are combined from two experiments with a total of nine mice/group. Value of $p = 0.14$ for the number of MHC class II^{high} $CD11c^+$ cells in draining lymph nodes of wild-type vs $cd73^{-/-}$ mice, and $p = 0.034$ for the comparison of total cell numbers/lymph node.

to induce DC migration to draining lymph nodes through the lymphatics and also their maturation and cytokine production (13). Because previous reports showed that Ado is one of the key regulators of DC function (43, 44), we speculated that the hypertrophied draining lymph nodes in $cd73^{-/-}$ mice might be due to increased migration of DC though the lymphatics. Therefore, we measured the absolute numbers of MHC class II^{high} $CD11c^+$ DC in the draining lymph nodes of wild-type and $cd73^{-/-}$ mice 6 h after the injection of LPS (Fig. 4*A*). As expected, the numbers of DC were increased in the draining lymph nodes of both strains of mice compared with those on the contralateral side. There was a trend toward higher numbers of DC in the draining lymph nodes of $cd73^{-/-}$ mice, because the average number was almost 50% higher than for wild-type mice; however, this difference was not statistically significant ($p = 0.14$). Nevertheless, these data suggest that increased cytokine production by DC could contribute to the larger size of draining lymph nodes in $cd73^{-/-}$ mice. It is interesting to note that the draining lymph nodes in the $cd73^{-/-}$ mice were significantly larger than those of wild-type mice ($p = 0.034$) even at this early time point (Fig. 4*B*), suggesting that the kinetics of the inflammatory response are accelerated when CD73 is absent.

Up-regulation of CD73 and $A_{2B}AR$ on HEV after an inflammatory stimulus

Previous studies showed CD73 expression can be regulated on HUVEC by mediators that are released during an inflammatory response, such as TNF-α (45), IFN-α (46), and Ado (47). Flow cytometry revealed a slight up-regulation of cell surface CD73 on CD45$^-$ PNAd$^+$ cells in draining lymph nodes relative to its level on HEV from control lymph nodes (Fig. 5*A*). Due to the lack of specific AR Abs suitable for flow cytometry, we used KOP2.16, a cell line derived from lymph node endothelial cells, and semiquantitative RT-PCR to examine the regulation of AR expression. Similar to what we observed in the HEV cDNA library (Fig. 1*D*), KOP2.16 expressed only the $A_{2B}AR$. Expression increased 3- to 5-fold 3 h after TNF-α stimulation in two independent experiments (Fig. 5*B*). These results suggest that elevated Ado, known to occur at sites of inflammation, could trigger the A_{2B}AR on HEV in draining lymph nodes, and that this could play a role in regulating lymphocyte migration into these nodes.

AR stimulation inhibits the increased lymphocyte migration into draining lymph nodes of CD73-deficient mice

Our previous findings and those of others suggest that Ado generated extracellularly by CD73 can modulate endothelial cell

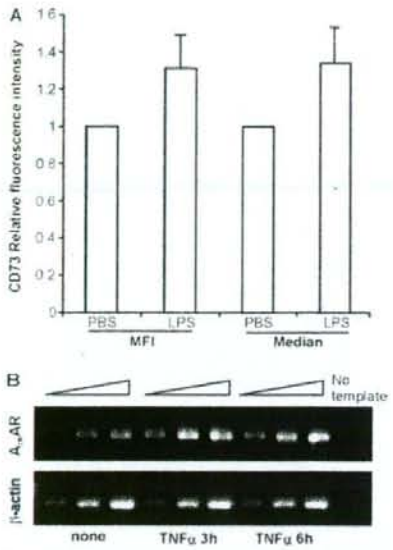

FIGURE 5. CD73 and the $A_{2B}AR$ are up-regulated on HEV after an inflammatory stimulus. *A*, LPS (1 μg) was injected into the left front footpad of $cd73^{+/+}$ mice, and an equivalent volume of PBS was injected into the right front footpad. Twenty-four hours later, lymph nodes were digested with collagenase, DNase I, and trypsin, as described in *Materials and Methods*, and cells were stained with allophycocyanin anti-CD45, purified anti-PNAd plus Alexa Fluor 488 anti-IgM, and biotinylated anti-CD73 plus PE-streptavidin. HEV were identified as $CD45^-$ $PNAd^+$ cells. The relative mean (MFI) and median fluorescence intensities for CD73 staining are shown (mean ± SD, total $n = 8$ from three independent experiments, $p < 0.01$ for MFI, and $p < 0.02$ for median fluorescence intensities in paired t tests comparing $PNAd^-$ cells from inflamed and control lymph nodes). *B*, KOP2.16 cells were cultured ± TNF-α for 3–6 h. RNA was isolated and $A_{2B}AR$ expression was determined by semiquantitative RT-PCR on 5-fold serial dilutions of cDNA using β-actin expression as an internal standard. Data are representative of one of two experiments. Quantitation of the band intensities revealed a 5-fold increase in $A_{2B}AR$ mRNA at 3 h and a 2.5-fold increase at 6 h relative to β-actin expression.

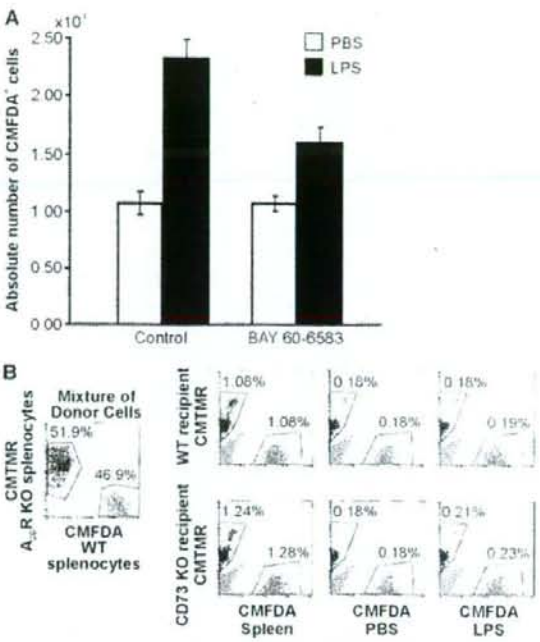

FIGURE 6. The A_{2B} AR agonist, BAY 60-6583, inhibits the increased lymphocyte migration into draining lymph nodes of CD73-deficient mice. *A*, LPS (1 μg) was injected into the left front footpad of $cd73^{+/+}$ and $cd73^{-/-}$ mice, and an equivalent volume of PBS was injected into the right front footpad. Twenty-two hours and 30 min after the LPS injection, the mice were injected i.v. with BAY 60-6583 (320 μg/kg) or an equivalent volume of diluted PEG 400 carrier, and 30 min later with 10^7 CMFDA-labeled $cd73^{+/+}$ splenocytes. One hour after the injection of labeled splenocytes, lymph nodes were harvested, the total numbers of cells in each lymph node were counted, and the percentages of $CMFDA^+$ cells were determined by flow cytometry ($n = 20$–26; $p = 0.0034$ for diluted PEG 400 vs BAY 60-6583 in draining lymph nodes; data combined from four separate experiments). *B*, LPS (1 μg) was injected into the left front footpad of wild-type and $cd73^{-/-}$ mice, and an equivalent volume of PBS was injected into the right front footpad (five mice/group). Twenty-three hours later, the mice were injected i.v. with an equal mixture of 10^7 wild-type and $A_{2B}R^{-/-}$ splenocytes labeled with CMFDA or CMTMR, respectively. One hour later, brachial lymph nodes were harvested, and the percentages of $CMFDA^+$ and $CMTMR^+$ lymphocytes were determined by flow cytometry. Data are representative of one of two experiments.

adhesion molecule expression and permeability via the A_{2A}AR and A_{2B}AR (27–30). Based on these findings, and our own observation that the A_{2B}R was the only AR expressed on HEV, we asked whether the A_{2B}AR-specific agonist BAY 60-6583 could influence lymphocyte homing after an inflammatory stimulus. As shown in Fig. 6*A*, treatment with BAY 60-6583 markedly decreased ($p = 0.0034$) the number of lymphocytes that migrated into the draining lymph nodes of CD73-deficient mice. There was no impact on lymphocyte migration into lymph nodes on the contralateral side. The effect of BAY 60-6583 on lymphocyte migration into draining lymph nodes of wild-type mice was much more modest and did not reach statistical significance (data not shown), perhaps because of higher concentrations of endogenous Ado in these mice. All of these results support our hypothesis that CD73-generated Ado serves to regulate lymphocyte migration into draining lymph nodes after an inflammatory stimulus at least in part by triggering A_{2B}AR signaling on HEV. Consistent with this hypothesis, $A_{2B}AR^{+/+}$ and $A_{2B}AR^{-/-}$ lymphocytes showed equivalent rates of lymphocyte migration into draining lymph nodes of LPS-treated wild-type and $cd73^{-/-}$ mice (Fig. 6*B*).

Discussion

Lymphocyte homing to peripheral lymph nodes depends on interactions with HEV, specialized blood vessels that express chemokines, and adhesion molecules required for lymphocyte transmigration. Although numerous reports have demonstrated the importance of L-selectin, PNAd, LFA-1, ICAM-1, and specific chemokines and chemokine receptors in the steady state, the way in which lymphocyte migration across HEV is regulated during an inflammatory response is not fully understood. The goal of this investigation was to determine whether CD73, which is expressed on both $PNAd^+$ endothelial cells and the basal lamina comprising HEV, plays a role in this process. The source of CD73 expressed on basal lamina is not known. However, CD73 is a GPI-anchored protein, and previous studies by Mehul et al. (48) showed that CD73 can bind to laminin, one of the components of the basal lamina. Therefore, we hypothesize that CD73 may be synthesized in cells such as endothelial cells, cleaved from the cell surface by

a phospholipase, and then bind to a component of the basal lamina such as laminin.

The contribution of CD73 to the formation of extracellular Ado, a well-known anti-inflammatory mediator, has been revealed in several experimental models. For example, the anti-inflammatory action of methotrexate in the carrageenan-treated air pouch model of inflammation is dependent upon CD73 (49). Similarly, CD73-generated Ado is necessary for ischemic preconditioning in both the heart (40) and kidney (50), and protects mice from bleomycin-induced lung injury (51). Furthermore, *cd73*-deficient mice exhibit a vascular leak syndrome characterized by neutrophil infiltration into tissues when exposed to normobaric hypoxia, suggesting a critical role for CD73-generated Ado in vascular barrier function (27–29). In contrast, several in vitro studies suggested that CD73 functions as a costimulatory molecule on T lymphocytes (33, 34) and an adhesion molecule that is important for lymphocyte binding to endothelium (35). The possibility that CD73 could impact lymphocyte interactions with HEV by multiple mechanisms prompted us to examine the role of this molecule in lymphocyte homing to lymph nodes. We showed in this study that Ado generated by CD73 on HEV negatively regulates lymphocyte migration from the bloodstream into LPS-induced draining lymph nodes. Because $cd73^{+/+}$ and $cd73^{-/-}$ splenocytes showed equivalent rates of migration into draining lymph nodes, it is unlikely that any signaling or adhesive function of CD73 on lymphocytes plays a role in regulating migration of lymphocytes across HEV.

Although no abnormalities were observed in the cellularity of lymphoid organs of $cd73^{-/-}$ mice or in the migratory capacity of $cd73^{-/-}$ lymphocytes under steady-state conditions, $cd73^{-/-}$ mice had larger draining lymph nodes when LPS, a TLR4 agonist, was injected into a local site. Short-term assays with CMFDA-labeled lymphocytes administered i.v. showed increased rates of migration into the draining lymph nodes of $cd73^{-/-}$ mice. This observation, coupled with the forward vs side scatter profile of the lymphocytes (our unpublished data), suggested that the lymph node hypertrophy induced by LPS was not due to the proliferation of lymphocytes, but rather to the accumulation of nondividing lymphocytes. Furthermore, anti-L-selectin Ab treatment demonstrated that CD73 modulates lymphocyte migration into draining lymph nodes by an L-selectin-dependent pathway. Interestingly, both T and B lymphocyte entrance was promoted in $cd73^{-/-}$ mice, suggesting that a common pathway for both cell types is modulated by CD73. In addition, the percentages of $CD73^+$ and $CD73^-$ lymphocytes did not change when splenocytes from $cd73^{+/+}$ mice were used as donors in migration experiments in $cd73^{+/+}$ mice, indicating that the ability to migrate across HEV was not influenced by the CD73 expression status of lymphocytes. Furthermore, the migration of splenocytes from $cd73^{+/+}$ and $cd73^{-/-}$ mice into draining lymph nodes of $cd73^{-/-}$ mice was comparable, demonstrating that CD73 expression on lymphocytes cannot compensate for a lack of CD73 on HEV.

Information in the literature concerning the regulation of endothelial CD73 expression by proinflammatory cytokines is conflicting. For example, Kalsi et al. (45) showed a decrease in its expression and in its enzyme activity after TNF-α treatment of HUVEC. In contrast, Niemela et al. (46) demonstrated that IFN-α and IFN-γ, but not other inflammatory cytokines such as IL-1β, IL-4, or TNF-α, could increase CD73 expression on HUVEC. Furthermore, Ado has been implicated in an increase in CD73 expression in microvascular endothelial cells that is mediated by a paracrine pathway (47). Our experiments revealed that the expression of CD73 on HEV in draining lymph nodes is up-regulated compared with HEV in the contralateral side. Although our analysis has the advantage of evaluating changes in CD73 expression in vivo, the mechanism by which CD73 expression is modulated is still unknown.

To determine whether the enhanced lymphocyte migration in *cd73*-deficient mice was caused by a lack of AR signaling, we treated mice with the $A_{2B}R$ agonist BAY 60-6583. This approach was taken because of the four known subtypes of AR; only the $A_{2B}AR$ was found in a cDNA library derived from $PNAd^+$ cells or in cDNA from the HEV-like cell line KOP2.16 (36). We also observed an up-regulation of $A_{2B}AR$ expression in KOP2.16 cells after exposure to TNF-α. Indeed, BAY 60-6583 treatment markedly reduced the rate of migration of labeled splenocytes into draining lymph nodes of $cd73^{-/-}$ mice. These data are consistent with the hypothesis that the $A_{2B}AR$ is at least partially responsible for the regulation of lymphocyte migration across HEV by CD73-generated Ado. Furthermore, the Ado is most likely derived from CD73 on HEV, because lymphocytes from $cd73^{+/+}$ and $cd73^{-/-}$ mice show similar increased rates of migration across HEV in draining lymph nodes of $cd73^{-/-}$ mice (i.e., Ado produced by $cd73^{-/-}$ lymphocytes does not appear able to trigger AR on HEV to regulate lymphocyte migration). Similarly, lymphocytes from $A_{2B}R^{+/+}$ and $A_{2B}R^{-/-}$ mice showed similar rates of migration into draining lymph nodes of wild-type mice, suggesting that it is triggering of the $A_{2B}R$ on HEV that is relevant.

The expression of the adhesion molecules ICAM-1 and VCAM-1 is normal on $cd73^{-/-}$ HEV in the steady state (our unpublished data). Our findings differ from those in a previous report (30), which concluded that CD73 deficiency resulted in increased VCAM-1 expression and decreased ICAM-1 expression on carotid arteries due to the lack of $A_{2A}AR$ signaling. This discrepancy could be explained by the fact that different cell types were being examined and that the $A_{2B}AR$, rather than the $A_{2A}AR$, seems to be the predominant AR on HEV. We did find that VCAM-1, but not ICAM-1, expression was up-regulated on HEV in draining lymph nodes after LPS administration and this effect was more pronounced in $cd73^{-/-}$ mice. However, neither anti-VLA-4 nor anti-VCAM-1 Ab treatment reversed the increased rates of lymphocyte migration into draining lymph nodes of $cd73^{-/-}$ mice after LPS treatment (our unpublished data), suggesting that the increase in VCAM-1 expression did not augment cell adhesion between lymphocytes and HEV. Furthermore, although the migration of CMFDA-labeled lymphocytes to draining lymph nodes was inhibited by treatment with an anti-LFA-1 Ab, the effect was the same in both $cd73^{+/+}$ and $cd73^{-/-}$ mice (our unpublished data). Taken together, these data support the conclusion that increased lymphocyte migration into draining lymph nodes of *cd73*-deficient mice is not mediated by increases in cell adhesion.

We propose instead that Ado generated by endothelial cell (and/or basal lamina) CD73 regulates lymphocyte migration across HEV through $A_{2B}AR$ signaling. The $A_{2B}AR$ is a seven-transmembrane-spanning G protein-coupled receptor that is coupled to G_s and uses cAMP as a second messenger (52). It has been firmly established that cAMP can modulate endothelial cell–cell junctions through the protein kinase A and/or Epac-Rap1 pathways (53, 54). Other reports suggest that the $A_{2B}AR$ can also be coupled to G_q (55). In the 1970s, several studies concluded that lymph node vasculature changed within 24 h after an inflammatory stimulus, and that this was associated with changes in vascular integrity (56, 57). Our studies do not address the mechanisms by which rates of lymphocyte migration are increased after an inflammatory stimulus, but do suggest that CD73-generated Ado may trigger a feedback mechanism to keep increases in permeability under control. Additional experiments with endothelial cell lines will be required to determine whether AR signaling modulates the ability of lymphocytes to migrate across HEV through changes in myosin L chain

phosphorylation and decreased formation of stress fibers and/or through Rap1/Epac-mediated increases in VE-cadherin-based cell-cell contacts. Future work will also address the consequences of increased lymphocyte migration into *cd73*$^{-/-}$ draining lymph nodes during an immune response.

Acknowledgments

We acknowledge Mary Flynn for manuscript preparation, the excellent technical assistance of Scott Hooker and Patrick Marble, and the expertise of Julie Maier in the Oklahoma Medical Research Foundation Imaging Facility. We also thank Dr. Paul Kincade for critical comments during manuscript preparation, Dr. Rob Welner for assistance with i.v. injections, and Drs. Almut Grenz and Tobias Eckle for advice regarding the administration of BAY 60-6583.

Disclosures

Thomas Krahn is an employee of Bayer HealthCare, the manufacturer of BAY 60-6583. All other authors have no conflicting financial interests.

References

1. Kraal, G., and R. E. Mebius. 1997. High endothelial venules: lymphocyte traffic control and controlled traffic. *Adv. Immunol.* 65: 347–395.
2. Miyasaka, M., and T. Tanaka. 2004. Lymphocyte trafficking across high endothelial venules: dogmas and enigmas. *Nat. Rev. Immunol.* 4: 360–370.
3. Rosen, S. D. 2001. Ligands for L-selectin: homing, inflammation, and beyond. *Annu. Rev. Immunol.* 22: 129–156.
4. Hamann, A., D. Jablonski-Westrich, A. Duijvestijn, E. C. Butcher, H. Baisch, R. Harder, and H. G. Thiele. 1988. Evidence for an accessory role of LFA-1 in lymphocyte-high endothelium interaction during homing. *J. Immunol.* 140: 693–699.
5. Campbell, J. J., J. Hedrick, A. Zlotnik, M. A. Siani, D. A. Thompson, and E. C. Butcher. 1998. Chemokines and the arrest of lymphocytes rolling under flow conditions. *Science* 279: 381–384.
6. Arbones, M. L., D. C. Ord, K. Ley, H. Ratech, C. Maynard-Curry, G. Otten, D. J. Capon, and T. F. Tedder. 1994. Lymphocyte homing and leukocyte rolling and migration are impaired in L-selectin-deficient mice. *Immunity* 1: 247–260.
7. Berlin-Rufenach, C., F. Otto, M. Mathies, J. Westermann, M. J. Owen, and A. Hamann. 1999. Lymphocyte migration in lymphocyte function-associated antigen (LFA)-1-deficient mice. *J. Exp. Med.* 189: 1467–1478.
8. Uchimura, K., J.-M. Gauguet, M. S. Singer, D. Tsay, R. Kannagi, T. Muramatsu, U. H. von Adrian, and S. D. Rosen. 2005. A major class of L-selectin ligands is eliminated in mice deficient in two sulfotransferases expressed in high endothelial venules. *Nat. Immunol.* 6: 1105–1113.
9. Butcher, E. C., M. Williams, K. Youngman, L. Rott, and M. Briskin. 1999. Lymphocyte trafficking and regional immunity. *Adv. Immunol.* 72: 209–253.
10. Mitoma, J., X. Bao, B. Petryniak, P. Schaerli, J. M. Gauguet, S. Y. Yu, H. Kawashima, H. Saito, K. Ohtsubo, J. D. Marth, et al. 2007. Critical functions of N-glycans in L-selectin-mediated lymphocyte homing and recruitment. *Nat. Immunol.* 8: 409–418.
11. Takeda, K., T. Kaisho, and S. Akira. 2003. Toll-like receptors. *Annu. Rev. Immunol.* 21: 335–376.
12. Rouke, J. A., A. S. Rao, P. J. Morris, C. P. Larsen, D. F. Hankins, and J. M. Austyn. 1995. Dendritic cell loss from nonlymphoid tissues after systemic administration of lipopolysaccharide, tumor necrosis factor, and interleukin 1. *J. Exp. Med.* 181: 2237–2247.
13. Tsujimoto, H., T. Uchida, P. A. Efron, P. O. Scumpia, A. Verma, T. Matsumoto, S. K. Tschoeke, R. F. Ungaro, S. Ono, S. Seki, et al. 2008. Flagellin enhances NK cell proliferation and activation directly and through dendritic cell-NK cell interactions. *J. Leukoc. Biol.* 78: 888–897.
14. Soderberg, K. A., G. W. Payne, A. Sato, R. Medzhitov, S. S. Segal, and A. Iwasaki. 2005. Innate control of adaptive immunity via remodeling of lymph node feed arteriole. *Proc. Natl. Acad. Sci. USA* 102: 16315–16320.
15. Webster, B., I. H. Ekland, L. M. Agle, S. Chyou, R. Ruggieri, and T. T. Lu. 2006. Regulation of lymph node vascular growth by dendritic cells. *J. Exp. Med.* 203: 1903–1913.
16. Thompson, L. F., J. M. Ruedi, A. Glass, G. Moldenhauer, P. Moller, M. G. Low, M. R. Klemens, M. Massaia, and A. H. Lucas. 1990. Production and characterization of monoclonal antibodies to the glycosyl phosphatidylinositol-anchored lymphocyte differentiation antigen ecto-5′-nucleotidase (CD73). *Tissue Antigens* 35: 9–19.
17. Linden, J. 2001. Molecular approach to adenosine receptors: receptor-mediated mechanisms of tissue protection. *Annu. Rev. Pharmacol. Toxicol.* 41: 775–787.
18. Franco, R., A. Valenzuela, C. Lluis, and J. Blanco. 1998. Enzymatic and extracellular role of ecto-adenosine deaminase in lymphocytes. *Immunol. Rev.* 161: 27–42.
19. Dong, R. P., J. Kameoka, M. Hegen, T. Tanaka, X. H. Xu, S. F. Schlossman, and C. Morimoto. 1996. Characterization of adenosine deaminase binding to human CD26 on T cells and its biologic role in immune response. *J. Immunol.* 156: 1349–1355.
20. Hashikawa, T., S. W. Hooker, J. G. Maj, C. J. Knott-Craig, M. Takedachi, S. Murakami, and L. F. Thompson. 2004. Regulation of adenosine receptor engagement by ecto-adenosine deaminase. *FASEB J.* 18: 131–133.
21. Sun, D. L. C. Samuelson, T. Yang, Y. Huang, A. Paliege, T. Saunders, J. Briggs, and J. Schnermann. 2001. Mediation of tubuloglomerular feedback by adenosine: evidence from mice lacking adenosine 1 receptors. *Proc. Natl. Acad. Sci. USA* 98: 9983–9988.
22. Ledent, C., J.-M. Vaugeois, S. N. Schiffmann, T. Pedrazzini, M. El Yacoubi, J.-J. Vanderhaeghen, J. Costentin, J. K. Heath, G. Vassart, and M. Parmentier. 1997. Aggressiveness, hypoalgesia and high blood pressure in mice lacking the adenosine A_{2a} receptor. *Nature* 388: 674–678.
23. Chen, J. F., Z. Huang, J. Ma, J. Zhu, R. Moratalla, D. Standaert, M. A. Moskowitz, J. S. Fink, and M. A. Schwarzschild. 1999. A_{2A} adenosine receptor deficiency attenuates brain injury induced by transient focal ischemia in mice. *J. Neurosci.* 19: 9192–9200.
24. Yang, D., Y. Zhang, H. G. Nguyen, M. Koupenova, A. K. Chauhan, M. Makitalo, M. R. Jones, C. St. Hilaire, D. C. Seldin, P. Toselli, et al. 2006. The A2B adenosine receptor protects against inflammation and excessive vascular adhesion. *J. Clin. Invest.* 116: 1913–1923.
25. Salvatore, C. A., S. L. Tilley, A. M. Latour, D. S. Fletcher, B. H. Koller, and M. A. Jacobson. 2000. Disruption of the A_3 adenosine receptor gene in mice and its effect on stimulated inflammatory cells. *J. Biol. Chem.* 275: 4429–4434.
26. Cronstein, B. N. 1994. Adenosine, an endogenous anti-inflammatory agent. *J. Appl. Physiol.* 76: 5–13.
27. Thompson, L. F., H. K. Eltzschig, J. C. Ibla, C. J. Van De Wiele, R. Resta, J. C. Morote-Garcia, and S. P. Colgan. 2004. Crucial role for ecto-5′-nucleotidase (CD73) in vascular leakage during hypoxia. *J. Exp. Med.* 200: 1395–1405.
28. Eltzschig, H. K., L. F. Thompson, J. Karhausen, R. J. Cotta, J. C. Ibla, S. C. Robson, and S. P. Colgan. 2004. Endogenous adenosine produced during hypoxia attenuates neutrophil accumulation: coordination by extracellular nucleotide metabolism. *Blood* 104: 3986–3992.
29. Eckle, T., M. Faigle, A. Grenz, S. Laucher, L. F. Thompson, and H. K. Eltzschig. 2008. A2B adenosine receptor dampens hypoxia-induced vascular leak. *Blood* 111: 2024–2035.
30. Zernecke, A., K. Bidzhekov, B. Ozuyaman, L. Fraemohs, E. A. Liehn, J. M. Luscher-Firzlaff, B. Luscher, J. Schrader, and C. Weber. 2006. CD73/ecto-5′-nucleotidase protects against vascular inflammation and neointima formation. *Circulation* 113: 2120–2127.
31. Resta, R., Y. Yamashita, and L. F. Thompson. 1998. Ecto-enzyme and signaling functions of lymphocyte CD73. *Immunol. Rev.* 161: 95–109.
32. Airas, L., J. Niemela, and S. Jalkanen. 2000. CD73 engagement promotes lymphocyte binding to endothelial cells via a lymphocyte function-associated antigen-1-dependent mechanism. *J. Immunol.* 165: 5411–5417.
33. Massaia, M., L. Perrin, A. Bianchi, J. Ruedi, C. Attisano, D. Altieri, G. J. Rijkers, and L. F. Thompson. 1988. Human T cell activation: synergy between CD73 (ecto-5′-nucleotidase) and signals delivered through CD3 and CD2 molecules. *J. Immunol.* 145: 1661–1671.
34. Dianzani, U., V. Redoglia, M. Bragardo, C. Attisano, A. Bianchi, D. DiFranco, G. Ramenghi, H. Wolff, L. L. Thompson, A. Pileri, and M. Massaia. 1993. Co-stimulatory signal delivered by CD73 molecule to human CD45RA^{hi}CD45RO$^{-/lo}$ (naive) CD8$^+$ T lymphocytes. *J. Immunol.* 151: 3961–3970.
35. Airas, L., J. Hellman, M. Salmi, P. Bono, I. Puurunen, D. J. Smith, and S. Jalkanen. 1995. CD73 is involved in lymphocyte binding to the endothelium: characterization of lymphocyte vascular adhesion protein 2 identifies it as CD73. *J. Exp. Med.* 182: 1603–1608.
36. Toyama-Sorimachi, N., K. Miyake, and M. Miyasaka. 1995. Activation of CD44 induces ICAM-1/LFA-1-independent, Ca^{++}, Mg^{++}-independent adhesion pathway in lymphocyte-endothelial cell interaction. *Eur. J. Immunol.* 25: 439–446.
37. Umemoto, E., T. Tanaka, H. Kanda, S. Jin, K. Tohya, K. Otani, K. Matsutani, M. Matsumoto, Y. Ebisuno, M. H. Jang, et al. 2006. Nepmucin, a novel HEV sialomucin, mediates L-selectin-dependent lymphocyte rolling and promotes lymphocyte adhesion under flow. *J. Exp. Med.* 203: 1603–1614.
38. Van De Wiele, C. J., J. G. Vaughn, M. R. Blackburn, C. Ledent, M. Jacobson, H. Jiang, and L. F. Thompson. 2002. Adenosine kinase inhibition promotes survival of fetal adenosine deaminase-deficient thymocytes by blocking dATP accumulation. *J. Clin. Invest.* 110: 395–402.
39. Yamashita, Y., S. W. Hooker, H. Jiang, A. B. Laurent, R. Resta, K. Khare, A. Coe, P. W. Kincade, and L. F. Thompson. 1998. CD73 expression and Fyn-dependent signaling on murine lymphocytes. *Eur. J. Immunol.* 28: 2981–2990.
40. Eckle, T., F. Krahn, A. Grenz, D. Kohler, M. Mittelbronn, C. Ledent, M. Jacobson, H. Osswald, L. F. Thompson, K. Unertl, and H. K. Eltzschig. 2007. Cardioprotection by ecto-5′-nucleotidase (CD73) and A2B adenosine receptors. *Circulation* 115: 1581–1590.
41. Kobie, J. J., P. R. Shah, L. Yang, J. A. Rebhahn, D. J. Fowell, and T. R. Mosmann. 2006. T regulatory and primed uncommitted CD4 T cells express CD73, which suppresses effector CD4 T cells by converting 5′-adenosine monophosphate to adenosine. *J. Immunol.* 177: 6780–6786.
42. Lepault, F., M. C. Gagnerault, C. Faveeuw, and C. Boitard. 1991. Recirculation, phenotype and functions of lymphocytes in mice treated with monoclonal antibody MEL-14. *Eur. J. Immunol.* 21: 3106–3112.
43. Panther, E., M. Idzko, Y. Herouy, H. Rheinen, P. J. Gebicke-Haerter, C. Mrowietz, S. Dichmann, and J. Norgauer. 2001. Expression and function of adenosine receptors in human dendritic cells. *FASEB J.* 15: 1965–1970.
44. Panther, E., S. Corinti, M. Idzko, Y. Herouy, M. Napp, A. La Sala, G. Girolomoni, and J. Norgauer. 2003. Adenosine affects expression of membrane molecules, cytokine and chemokine release, and the T-cell stimulatory capacity of human dendritic cells. *Blood* 101: 3985–3990.
45. Kalsi, K., C. Lawson, M. Dominguez, P. Taylor, M. H. Yacoub, and R. T. Smolenski. 2002. Regulation of ecto-5′-nucleotidase by TNF-α in human endothelial cells. *Mol. Cell. Biochem.* 232: 113–119.

46. Niemela, J., T. Henttinen, G. G. Yegutkin, L. Airas, A. M. Kujari, P. Rajala, and S. Jalkanen. 2004. IFN-α induced adenosine production on the endothelium: a mechanism mediated by CD73 (ecto-5′-nucleotidase) up-regulation. *J. Immunol.* 172: 1646–1653.

47. Narravula, S., P. F. Lennon, B. U. Mueller, and S. P. Colgan. 2000. Regulation of endothelial CD73 by adenosine: paracrine pathway for enhanced endothelial barrier function. *J. Immunol.* 165: 5262–5268.

48. Mehul, B., M. Dosvnette-Mayne, M. Aubery, H. Mannherz, and P. Codogno. 1990. 5′-Nucleotidase is involved in chick embryo myoblast spreading on laminin. *Cell Biol. Int. Rep.* 2: 155–164.

49. Montesinos, M. C., M. Takedachi, L. F. Thompson, T. F. Wilder, P. Fernández, and B. N. Cronstein. 2007. The anti-inflammatory mechanism of methotrexate depends on extracellular conversion of adenine nucleotides to adenosine by ecto-5′-nucleotidase: findings in a study of ecto-5′-nucleotidase gene-deficient mice. *Arthritis Rheum.* 56: 1440–1445.

50. Grenz, A., H. Zhang, T. Eckle, M. Mittelbronn, M. Wehrmann, C. Köhle, D. Cloor, L. F. Thompson, H. Osswald, and H. K. Eltzschig. Protective role of ecto-5′-nucleotidase (CD73) in renal ischemia. *J. Am. Soc. Nephrol.* 18: 833–845.

51. Volmer, J. B., L. F. Thompson, and M. R. Blackburn. 2006. Ecto-5′-nucleotidase (CD73)-mediated adenosine production is tissue protective in a model of bleomycin-induced lung injury. *J. Immunol.* 176: 4449–4458.

52. Schulte, G., and B. B. Fredholm. 2003. The G_s-coupled adenosine A_{2B} receptor recruits divergent pathways to regulate ERK1/2 and p38. *Exp. Cell Res.* 290: 168–176.

53. Fukuhara, S., A. Sakurai, H. Sano, A. Yamagishi, S. Somekawa, N. Takakura, Y. Saito, K. Kangawa, and N. Mochizuki. 2005. Cyclic AMP potentiates vascular endothelial cadherin-mediated cell-cell contact to enhance endothelial barrier function through an Epac-Rap1 signaling pathway. *Mol. Cell. Biol.* 25: 136–146.

54. Patterson, C. E., H. Lum, K. L. Schaphorst, A. D. Verin, and J. G. Garcia. 2000. Regulation of endothelial barrier function by the cAMP-dependent protein kinase. *Endothelium* 7: 287–308.

55. Linden, J., T. Thai, H. Figler, X. Jin, and A. S. Robeva. 1999. Characterization of human A_{2B} adenosine receptors: radioligand binding, Western blotting, and coupling to G_q in human embryonic kidney 293 cells and HMC-1 mast cells. *Mol. Pharmacol.* 56: 705–713.

56. Herman, P. G., I. Yamamoto, and H. Z. Mellins. 1972. Blood microcirculation in the lymph node during the primary immune response. *J. Exp. Med.* 136: 697–714.

57. Anderson, N. D., A. O. Anderson, and R. G. Wyllie. 1975. Microvascular changes in lymph nodes draining skin allografts. *Am. J. Pathol.* 81: 131–160.

Periodontal Tissue Regeneration Using Fibroblast Growth Factor -2: Randomized Controlled Phase II Clinical Trial

Masahiro Kitamura[1], Keisuke Nakashima[2], Yusuke Kowashi[2], Takeo Fujii[3], Hidetoshi Shimauchi[4], Takashi Sasano[4], Toshi Furuuchi[4], Mitsuo Fukuda[5], Toshihide Noguchi[5], Toshiaki Shibutani[6], Yukio Iwayama[6], Shogo Takashiba[7], Hidemi Kurihara[8], Masami Ninomiya[9], Jun-ichi Kido[9], Toshihiko Nagata[9], Takafumi Hamachi[10], Katsumasa Maeda[10], Yoshitaka Hara[11], Yuichi Izumi[12], Takao Hirofuji[13], Enyu Imai[14], Masatoshi Omae[15], Mitsuru Watanuki[16], Shinya Murakami[1]*

1 Osaka University Dental Hospital, Suita, Japan, **2** Dental Hospital, Health Sciences University of Hokkaido, Ishikari-Tobetsu, Japan, **3** Medical and Dental Clinic, Health Sciences University of Hokkaido, Sapporo, Japan, **4** Tohoku University Dental Hospital, Sendai, Japan, **5** Aichigakuin University Dental Hospital, Nagoya, Japan, **6** Asahi University Dental Hospital, Mizuho, Japan, **7** Okayama University Hospital of Dentistry, Okayama, Japan, **8** Hiroshima University Hospital of Dentistry, Hiroshima, Japan, **9** Tokushima University Dental Hospital, Tokushima, Japan, **10** Kyushu University Dental Hospital, Fukuoka, Japan, **11** Nagasaki University Hospital, Attached School of Dentistry, Nagasaki, Japan, **12** Kagoshima University Dental Hospital, Kagoshima, Japan, **13** Fukuoka Dental College Hospital, Fukuoka, Japan, **14** Osaka University Hospital, Suita, Japan, **15** Izumisano Municipal Hospital, Rinku General Medical Center, Izumisano, Japan, **16** Kaken Pharmaceutical Co., Ltd., Tokyo, Japan

Abstract

Background: The options for medical use of signaling molecules as stimulators of tissue regeneration are currently limited. Preclinical evidence suggests that fibroblast growth factor (FGF)-2 can promote periodontal regeneration. This study aimed to clarify the activity of FGF-2 in stimulating regeneration of periodontal tissue lost by periodontitis and to evaluate the safety of such stimulation.

Methodology/Principal Findings: We used recombinant human FGF-2 with 3% hydroxypropylcellulose (HPC) as vehicle and conducted a randomized double-blinded controlled trial involving 13 facilities. Subjects comprised 74 patients displaying a 2- or 3-walled vertical bone defect as measured ≥3 mm apical to the bone crest. Patients were randomly assigned to 4 groups: Group P, given HPC with no FGF-2; Group L, given HPC containing 0.03% FGF-2; Group M, given HPC containing 0.1% FGF-2; and Group H, given HPC containing 0.3% FGF-2. Each patient underwent flap operation during which we administered 200 μL of the appropriate investigational drug to the bone defect. Before and for 36 weeks following administration, patients underwent periodontal tissue inspections and standardized radiography of the region under investigation. As a result, a significant difference ($p = 0.021$) in rate of increase in alveolar bone height was identified between Group P (23.92%) and Group H (58.62%) at 36 weeks. The linear increase in alveolar bone height at 36 weeks in Group P and H was 0.95 mm and 1.85 mm, respectively ($p = 0.132$). No serious adverse events attributable to the investigational drug were identified.

Conclusions: Although no statistically significant differences were noted for gains in clinical attachment level and alveolar bone gain for FGF-2 groups versus Group P, the significant difference in rate of increase in alveolar bone height ($p = 0.021$) between Groups P and H at 36 weeks suggests that some efficacy could be expected from FGF-2 in stimulating regeneration of periodontal tissue in patients with periodontitis.

Trial Registration: ClinicalTrials.gov NCT00514657

Citation: Kitamura M, Nakashima K, Kowashi Y, Fujii T, Shimauchi H, et al. (2008) Periodontal Tissue Regeneration Using Fibroblast Growth Factor -2: Randomized Controlled Phase II Clinical Trial. PLoS ONE 3(7): e2611. doi:10.1371/journal.pone.0002611

Editor: William Giannobile, University of Michigan, United States of America

Received September 10, 2007; **Accepted** May 13, 2008; **Published** July 2, 2008

Funding: This study was supported by Kaken Pharmaceutical Co., Ltd., which proposed study protocol and was responsible for data collection and prespecified statistical analysis. Preparation of the manuscript was consigned to the authors and the views expressed in this article do not necessarily reflect those of Kaken Pharmaceutical Co., Ltd.

Competing Interests: SM received research grants from Kaken Pharmaceutical Co., Ltd. MW is an employee and stockholder of Kaken Pharmaceutical Co., Ltd.

* E-mail: ipshinya@dent.osaka-u.ac.jp

Introduction

Periodontitis, evoked by the bacterial biofilm (dental plaque) that forms around teeth, progressively destroys the periodontal tissue supporting the teeth, including the periodontal ligament, cementum, alveolar bone and gingiva. Ultimately, this chronic inflammatory disease can lead to loss of the affected teeth [1–3]. All over the world, this disease remains highly prevalent [4] and is considered to threaten quality of life (QOL) for middle-aged and older populations as far as "oral" functions are concerned. Some

success has been achieved in suppressing progression of periodontitis by mechanically removing bacterial biofilm, the very cause of the disease. However, removal of the cause, bacterial plaque, with conventional periodontal and/or surgical treatments can, at best, reduce pocket depth and diminish inflammation in the affected region. No such treatment can ever regenerate lost periodontal tissue or normal structure and functionality. Considering that the "mouth" and "teeth" have various aesthetic and functional roles to play, establishing a brand-new treatment that enables the regeneration and rebuilding of periodontal tissue once destroyed by periodontal disease represents a task of tremendous importance.

To regenerate periodontal tissue destroyed by periodontitis, the chain of events requires stimulation of cementoblasts and osteoblasts into differentiation on the dental root and alveolar bone surfaces facing the region of periodontal tissue defect, followed by regeneration of the cementum and alveolar bone. Collagen fascicles produced by the periodontal ligament fibroblasts should then be embedded into those regenerated hard tissues, to rebuild new tissue to support teeth. Researchers have recently confirmed the existence of mesenchymal stem cells within the periodontal ligament, one of the cornerstones of periodontal tissue. These stem cells can differentiate into cells such as cementoblasts and osteoblasts [5]. Using the biological potentials of those stem cells to stimulate the regeneration of periodontal tissue is now being recognized as clinically possible. Some researchers are already trying to establish new treatments to accelerate the regeneration of periodontal tissue by local application of human recombinant cytokines to stimulate proliferation and differentiation into hard-tissue forming cells of undifferentiated mesenchymal cells among periodontal ligament cells. Direct local application of a combination of factors such as platelet-derived growth factor (PDGF) and insulin-like growth factor (IGF)-I [6], bone morphogenetic protein (BMP)-2 [7,8], transforming growth factor (TGF)-β [9], osteogenic protein (OP)-1 [10] and brain-derived neurotrophic factor (BDNF) [11] to artificial defects in periodontal tissue made in laboratory animals reportedly stimulates and promotes regeneration of regional periodontal tissue. In addition, the efficacy of PDGF-BB plus β-tricalcium phosphate (β-TCP, an osteoconductive scaffold) for periodontal tissue regeneration in human has recently been reported [12].

Fibroblast growth factor (FGF)-2 displays potent angiogenic activity and mitogenic ability on mesenchymal cells. To date, FGF-2 has been reported as efficacious in regenerating periodontal tissue in models of artificial defect of periodontal tissue in beagles and non-human primates (*Macaca fascicularis*) and in a model of surgically created periodontitis in beagles [13–15].

The present clinical trial used hydroxypropylcellulose (HPC)-based FGF-2 as the investigational agent. The purpose of this trial was to both clarify the activity of FGF-2 to regenerate periodontal tissue in periodontitis patients and to confirm drug safety. This study was a randomized, double-blinded clinical trial (Phase II) involving placebos and multiple dental facilities in compliance with good clinical practice (GCP) guidelines, representing the first trial to examine the efficacy and safety of FGF-2 in periodontitis patients with concurrent control of dose-response relationships.

The periodontium that supports teeth displays a tissue structure wherein the alveolar bone (hard tissue surrounding dental roots) is covered by the gingiva (soft tissue), and "true regeneration" thus involves the regeneration of both hard and soft tissues. To improve tooth support, regenerating hard tissues including alveolar bone is crucial. Hence, in the present study, under the assumption that FGF-2 would regenerate both hard and soft tissues, the rate of increase in alveolar bone height was established as the most important outcome measure. Furthermore, to confirm soft-tissue regeneration, the millimeter of clinical attachment level (CAL) regained was added as a main outcome measure.

Including recruitment of subjects, the clinical trial was performed from December 1, 2001 to September 29, 2004.

Methods

The Protocol for this trial and supporting CONSORT checklist are available as supporting informations; see Checklist S1 and Protocol S1.

This was a randomized, double-blinded, clinical trial of dose responses including placebo comparison, involving 13 dental facilities. Study protocols were approved prior to initiation of the study by the institutional review boards of the respective participating facilities.

1. Participants

Patients with periodontitis visiting any of the 13 dental institutions listed in Table 1 were requested to participate. In compliance with GCP guidelines, prospective 91 patients who provided written informed consent underwent clinical inspection and oral cavity diagnosis. Among 91 patients 80 patients who satisfied the selection and exclusion criteria described in Tables 2 and 3 were finally registered. Each subject received a standard initial preparation, including oral hygiene instruction, full-mouth scaling and root planing before surgical treatment, to minimize bacterial insult and reduce variability between lesions at baseline. Using oral radiographs and periodontal tissue inspection results, regions of investigation were determined as 2- or 3-walled vertical periodontal tissue defects ≥3 mm apical to the remaining alveolar bone crest.

2. Interventions, Design and Procedure

This trial employed recombinant human FGF-2 (Code No. KCB-1; Kaken Pharmaceutical Co., Ltd., Tokyo, Japan) produced by genetic recombination that introduced the gene for human FGF-2 into *Escherichia coli*. To improve the operability of drug administration to the region of alveolar bone defect, before administration we mixed freeze-dried FGF-2 with 3% HPC, a colorless and viscid solution, and prepared the gel-like investigational drug for this clinical trial (Code No. KCB-1D). FGF-2 concentration in the investigational drug was then prepared to 0% (placebo), 0.03%, 0.1% or 0.3% and administered to the region of investigation within 2 h of preparation. Before the start and after completion of investigational drug administration, a third-party organization (University of Shizuoka, Shizuoka, Japan) measured FGF-2 concentrations for each group to ascertain that FGF-2 concentrations in vials were accurate according to good manufacturing practice standards.

The clinical trial was conducted according to the schedule shown in Figure 1. The 80 patients were registered at the Registration Center (Adjust Co., Ltd., Sapporo, Japan) and then randomly assigned to the following 4 groups: Group P, placebo group administered HPC containing no FGF-2; Group L, administered HPC containing 0.03% FGF-2; Group M, administered HPC containing 0.1% FGF-2; and Group H, administered HPC containing 0.3% FGF-2.

All flap operations were performed in accordance with the modified Widman procedure. The proposed surgical area was anesthetized using local anesthetic. Following intracrevicular incision, buccal and lingual full-thickness (mucoperiosteal) flaps were elevated. Following reflection of the mucoperiosteal flap, all granulation tissue associated with the bone defect was removed. Subgingival soft and hard deposits on the root surface were

Table 1. The 13 trial dental facilities and the investigators

Trial facilities	Investigators	Number of patients
Dental Hospital, Health Sciences University of Hokkaido	Yusuke Kowashi	4
Medical and Dental Clinic, Health Sciences University of Hokkaido	Takeo Fujii	9
Tohoku University Dental Hospital	Hidetoshi Shimauchi	6
Aichigakuin University Dental Hospital	Mitsuo Fukuda	7
Asahi University Dental Hospital	Toshiaki Shibutani	6
Osaka University Dental Hospital	Masahiro Kitamura	6
Okayama University Hospital of Dentistry	Shogo Takashiba	11
Hiroshima University Hospital of Dentistry	Hidemi Kurihara	3
Tokushima University Dental Hospital	Jun-ichi Kido	12
Kyushu University Dental Hospital	Takafumi Hamachi	2
Nagasaki University Hospital Attached School of Dentistry	Yoshitaka Hara	6
Kagoshima University Dental Hospital	Yuichi Izumi	8
Fukuoka Dental College Hospital	Takao Hirofuji	0
		80

doi:10.1371/journal.pone.0002611.t001

removed utilizing both hand and ultrasonic instrumentation to ensure thorough degranulation and root planing. After that, 200 μL of investigational drug was administered to the bone defect region described above. No specific root conditioning was performed.

Next, at 1, 2 and 4 weeks after administration, the same clinical inspections were performed as before administration, and anti-FGF-2 antibodies in serum 2 and 4 weeks after administration were measured. At 12, 24 and 36 weeks following administration, standardized radiographs were taken, periodontal tissues were inspected and subjective symptoms and objective findings were observed. In addition, 6 patients from each of the groups were randomly selected and blood samples were drawn. At 1, 2 and 4 h after administering the investigational drug, FGF-2 concentrations in serum were measured.

3. Randomization

An independent organization, the Registration Center (Adjust Co., Ltd., Sapporo, Japan), was used to keep treatment allocation inaccessible to any patients or other individuals involved in the trial. The Registration Center created an allocation table in which a block size of 4 cases per block was allocated to investigational drugs comprising placebo (Group P), 0.03% FGF-2 (Group L), 0.1% FGF-2 (Group M) or 0.3% FGF-2 (Group H). According to this allocation table, a label indicating the corresponding drug number was attached to each and every vial of drug. After drugs were allocated, the Registration Center sealed and kept the allocation table in confidence until the clinical trial was completed. Freeze-dried drugs for Groups P, L, M and H were indistinguishable based on appearance.

Investigators at each facility checked all inclusion and exclusion criteria and registered patients one at a time by faxing patient information obtained under informed consent to the Registration Center. The center again checked the documents to make sure that each subject had satisfied all inclusion and exclusion criteria, then randomly allocated subjects as necessary to receive drugs based on a single block consisting of one drug sample each from Groups P, L, M, and H. The assigned drug numbers were then faxed back to the investigators. The blind was not broken until this clinical trial was completely finished.

Table 2. Criteria for selecting subjects

1)	Those diagnosed as having, from radiography and other results, 2- or 3-walled vertical intrabony defect as being measured at ≥3 mm apical to the remaining alveolar bone crest
2)	Those who have accomplished initial preparation and have been showing good compliance
3)	Those with mobility of the tooth to investigate of Degree 2 or less and with width of attached gingiva for which the existing Guided Tissue Regeneration (GTR) treatment is considered appropriate (Those with no width of keratinized gingival is not eligible)
4)	Those for whom supportive periodontal treatment (SPT) is applicable, in accordance with usual post-operative procedures following flap operation and GTR treatment
5)	Those whose oral hygiene is well established and who are able to perform appropriate tooth brushing following instructions of the investigators and/or sub-investigators after investigational drug administration
6)	Those ≥20-years-old and <65-years-old
7)	Those who understand the purposes of the trial and are capable of making an independent decision to comply with trial requirements
8)	Those who are able to visit their hospitals in accordance with the trial schedule

We selected those patients who met the criteria listed above, from those who the investigators and/or sub-investigators determined were in need of flap operation.

doi:10.1371/journal.pone.0002611.t002

Table 3. Criteria for excluding subjects

1)	Those administered a calcium antagonist during the 4 weeks preceding administration of the investigational drug
2)	Those in need of administration of adrenal cortical steroid (equivalent to>20 mg/day of Predonin) within 4 weeks after investigational drug administration
3)	Those scheduled to undergo a surgical operation in the vicinity of the tooth to investigate within 36 weeks after investigational drug administration
4)	Those with coexisting mental or consciousness disorder
5)	Those with coexisting malignant tumour or history of the same
6)	Those with coexisting diabetes (HbA_{1C} >6.5%)
7)	Those in an extremely poor nutritional condition (serum albumin concentration <2 g/dL)
8)	Those with ≥200 mL of blood drawn during the 4 weeks preceding investigational drug administration
9)	Those administered another investigational drug during the 24 h preceding investigational drug administration
10)	Those with coexisting disorder of the kidney, liver, blood and/or circulatory system (Grade 2 or above)
11)	Those who are either pregnant, possibly pregnant or breast-feeding, or who hope to become pregnant during the period of the trial
12)	Those with a previous history of hypersensitivity to a protein drug
13)	Others who the investigators or sub-investigators determined as unsuitable for the trial

doi:10.1371/journal.pone.0002611.t003

4. Outcome measures

Main outcome measures prespecified in the study protocol comprised: rate of increase in alveolar bone height; and millimeter of CAL regained. In addition, we examined whether and to what extent adverse events emerged for which causal relationships with the investigational drug were not ruled out before breaking the blind. We set rate of increase in alveolar bone height as the most statistically important outcome (primary outcome). Probing depth (PD), bleeding on probing (BOP), gingival index (GI), tooth mobility (MO), gingival recession (REC), plaque index (PII), and width of keratinized gingiva (KG) were selected as secondary outcome measures.

1) Standardized radiography for regions of investigation

Our geometrically standardized radiography employed dental film (Kodak InSight Super Poly-Soft; Eastman Kodak Company, New York, USA) and photograph indicators (Cone Indicator-II; Hanshin Technical Laboratory, Nishinomiya, Japan) customized with resin stents.

Five doctors specializing in dental radiology from the Department of Oral Diagnosis at Tohoku University Graduate School of Dentistry independently measured rate of increase in alveolar bone height using the methods described in Figure 2. Errors caused by slight variation in angulations of X-ray imaging were corrected based on the distance between two immobile anatomical

Item	Before registration	Before administration	Administration	After administration: Hour 1	Hour 2	Hour 4	Hour 24	Date 2	Date 3	Week 1	Week 2	Week 4	Week 12	Week 24	Week 36
Patient agreement	●														
Registration	●														
Patient background	●	●													
Administration of investigational drug			●												
Radiography		●											●	●	●
Clinical attachment level		●											●	●	●
Periodontal tissue inspections		●											●	●	●
Subjective symptoms and objective findings		●						●		●	●	●	●	●	●
Clinical inspections	●	●								●	●	●			
Oral cavity inspection	●														
Anti-FGF-2 antibody in serum		●									●	●			
FGF-2 concentration in serum (n=6 from each group)		●		●	●	●	●								

Figure 1. Schedule of the clinical trial. We randomly allocated the 80 patients into 4 groups (n = 20 each): 1) a placebo group (Group P); 2) a group administered 0.03% FGF-2 (Group L); 3) a group administered 0.1% FGF-2 (Group M); and 4) a group administered 0.3% of FGF-2 (Group H). The clinical trial was then conducted in accordance with the clinical trial schedule. We also measured FGF-2 concentrations in the blood serum of 6 patients randomly chosen from each of the 4 groups, before and then 1 h, 2 h and 4 h after administration of the investigational drug.
doi:10.1371/journal.pone.0002611.g001

reference points. The median of 5 measurements taken from the same image was then selected for efficacy analysis. Before making measurements in the present study, X-ray images were read to measure intra- and interexaminer variations. Each of the 5 doctors measured the same sample 5 times to calculate coefficients of variation. The results showed that intra- and interexaminer coefficients of variation were both 3%, confirming the absence of marked variations.

2) Inspection of periodontal tissue around the tooth under investigation

We measured the items shown in Table 4 at 6 positions (mesiobuccal, buccal, distobuccal, mesiolingual, lingual and distolingual) around each tooth under investigation.

All examiners used PCP-UNC-15 periodontal probes (Hu-Friedy, Chicago, IL). We held meetings with each investigator from all of the participating facilities. In addition, a start-up meeting in which all investigators from a single facility participated was held at each facility. In these meetings, the protocol for this clinical trial was confirmed and clinical evaluations were standardized between facilities. In all facilities, the same person (MW) explained the detailed methods of probing inspections to all investigators and confirmed reproducibility and consistency for each investigator. Furthermore, prior to initiating baseline measurements, intra- and interexaminer calibrations were performed on patients at each facility to ensure reproducibility and consistency by each investigator. Each patient was examined by the same examiner at every recall visit throughout this clinical trial.

5. Safety evaluation

1) Observation of subjective symptoms and objective findings

Medical findings for both the oral cavity and whole body were confirmed by interview and visual inspection.

2) Clinical inspections

A clinical testing company (SRL Medisearch Inc., Tokyo, Japan) measured the inspection items (see Table S1 of supporting items). In cases where we discovered unusual changes in any of the clinical inspection values listed within 4 weeks after administration of the investigational drug, a follow-up survey was conducted.

3) Measurement of anti-FGF-2 antibody levels in serum

The Pharmacokinetics Department of Kaken Pharmaceutical Co., Ltd. measured levels of anti-FGF-2 antibody (IgG) in serum using ELISA.

4) Measurement of FGF-2 concentration within serum

The Metabolism Research Department of Kaken Pharmaceutical Co., Ltd. measured FGF-2 concentrations in serum using ELISA.

6. Sample size calculation

The effect of a combination drug comprising recombinant human PDGF-BB and IGF-I in humans on periodontal regeneration has already been reported [19]. In PDGF-BB/IGF-I-treated subjects (n = 16), mean (±standard error of mean) bone fill was 18.5±7% for control sites (surgery alone) and 42.3±9% for PDGF-BB/IGF-I sites with a mean difference of 23.8%. Assuming a rate of increase for placebo control of 20% (standard deviation, 28%) in alveolar bone of the defect region, the planned sample size

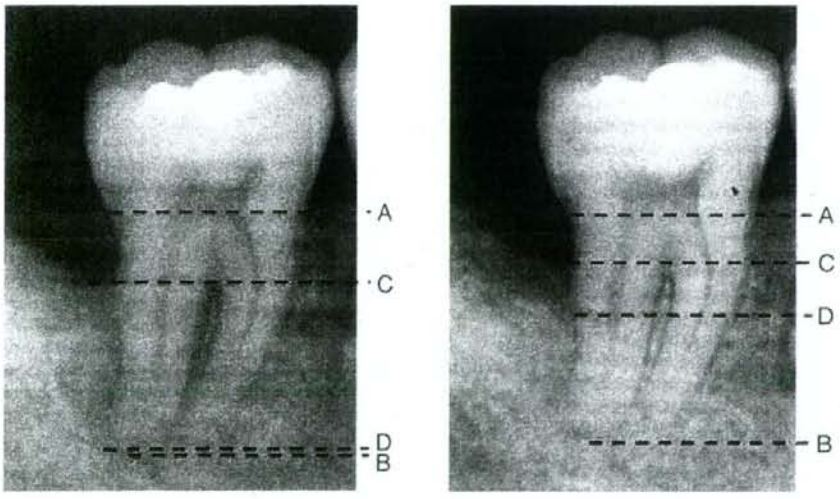

Figure 2. Measured points of alveolar bone height using standardized radiographs. Standardized dental radiographs taken before and after FGF-2 administration in one subject (a 29-year-old man) given 0.3% FGF-2. Points A, B, C and D represent the cementoenamel junction, apex, remaining alveolar bone crest and bottom of the bone defect, respectively. The examiners measured tooth axis heights between Points A and B, Points A and C, and Points A and D on the X-ray for each patient. To adjust for slight errors due to imaging, measurements for 5 examiners were multiplied by A-B ratio of before to after administration to correct A-B, A-C and A-D after administration (adjusted A-B, A-C and A-D, respectively). Rate of increase in alveolar bone height was derived from the following calculation formula. [(A-D before administration) - (adjusted A-D after administration)] by C-D before administration. On this radiography, C-D before administration, A-D before administration and, adjusted A-D after administration measured 9.00 mm, 12.80 mm and 5.93 mm, respectively. These values assigned to the above formula, we obtained the rate of increase in alveolar bone height as follows. The rate of increase in alveolar bone height (%) = 100(12.80–5.93)/9.00 = 76.35.
doi:10.1371/journal.pone.0002611.g002

Table 4. Periodontal tissue inspection

1)	Clinical attachment level (CAL): A stent was prepared for each subject. Using as the control point the cementoenamel junction or margin of the restorative material, distance between the control point and bottom of the gingival sulcus was measured for each test subject, using the same periodontal probe.
2)	Probing depth (PD): Simultaneously with CAL measurement, we measured distance from the gingival margin to the bottom of the gingival sulcus for each subject using the same periodontal probe.
3)	Bleeding on probing (BOP; + or −): The presence of bleeding was checked 10 s after probing.
4)	Gingival index (GI): GI was determined as described by Löe and Silness.[16]
5)	Mobility of tooth (MO): MO was determined as described by Miller.[17]
6)	Recession of gingiva (REC): Using as the control point the cementoenamel junction or margin of the restorative material, distance between the control point and gingival margin was measured for each subject, using the same periodontal probe.
7)	Plaque index (PII): PII was determined as described by Silness and Löe.[18]
8)	Width of keratinized gingiva (KG): The shortest distance between the coronal gingival margin and mucogingival junction was measured for each subject, using the same periodontal probe.

doi:10.1371/journal.pone.0002611.t004

of 20 patients in each group would provide 90% power to detect any clinically relevant treatment difference of 30% at a two-tailed significance level of 0.05.

7. Statistical methods

For analysis, we employed SAS version 8.2 software (SAS Institute Inc., Carey, North Carolina, USA). The level of statistical significance was set at $p<0.05$ in advance. Data analysis covered those patients administered the randomly allocated investigational drugs. In analyses concerning efficacy, those patients found to have either 1- or 4-walled intrabony defect during surgery after allocation were excluded. To statistically compare the 3 dose groups in terms of rate of increase in alveolar bone mass with the placebo group, the Dunnett option was used based on the Mixed procedure in the SAS system, in which adjusted p-values were computed for multiple comparisons, and analysis for rates of increase during follow-up was performed using repeated-measures analysis of variance with the Mixed procedure.

Results

1. Patient characteristics at the beginning of the trial (baseline characteristics)

Figure 3 shows flow of patients through the study. The 91 patients screened as subjects were consenting periodontitis patients for whom periodontal tissue regeneration therapy was indicated by investigators based on these criteria among a large number of potential subjects. Following the exclusion of 11 of these 91 patients, a final total of 80 patients were enrolled as subjects in the present clinical trial. The 11 patients were excluded due to findings on clinical inspection that could not have been determined by investigators during clinical periodontal diagnosis, or due to withdrawal of consent to participate. The 80 patients were then randomly assigned to 4 groups of 20 patients each. Table 5 shows the baseline characteristics of patients.

2. Evaluation of efficacy

Rate of increase in alveolar bone height at 12, 24 and 36 weeks after FGF-2 administration are shown in Table 6. A significant difference ($p=0.021$) was only identified between Group P and Group H at 36 weeks. The detailed data at 36 weeks are shown in Fig. 4 and Table 7. Adjusted mean differences from Group P were also calculated as least square mean (LSMean) differences based on two-way analysis of variance or analysis of covariance (data not shown). Adjusted mean differences for gender, site of investigational drug administration (maxilla or mandible), CAL, REC, GI, MO, PII and type of bone defect mostly resembled raw mean differences and the lower 95% confidence limits of LSMean difference (Group P vs. H) was above zero (0<lower 95% confidence limit). These results indicate that baseline characteristic imbalances between groups had no influence on evaluation of efficacy. Regarding the CAL regained (Table 8), REC, KG, MO and PII (see Table S2 of supporting items), no significant differences existed between the 4 groups. Although PD, GI and BOP prevalence all decreased with time following periodontal surgical treatment in the 4 groups (see Table S3 of supporting items), no significant differences were noted between these groups.

Two-way analysis of variance was used to assess facility differences in the 4 groups in the rate of increase in alveolar bone height, revealing no significant treatment-by-facility interaction ($p=0.795$). This suggests that no marked facility differences existed with respect to response.

3. Safety evaluation

Major adverse events for which causal relationships with the investigational drug were not ruled out before breaking the blind included positive urinary albumin, increased urinary excretion of β2-microglobulin and N-acetyl-beta-D-glucosamidase, increased serum creatine kinase and C-reactive protein and increased cases of hypersensitive dentine (see Table S4 of supporting items). Frequencies of these adverse events were independent of FGF-2 concentration. No serious adverse events were observed throughout the clinical trial period. A possible association was also considered between frequency of adverse events observed during the trial and the investigational drug administration. None of the adverse events exhibited a strong causal relationship or were severe, and except for one case, all events resolved without any special treatment. For each group, the presence/absence and frequency of adverse events were calculated. Fisher's exact test showed that group allocations exhibited no association to the presence/absence of adverse events ($p=0.469$). In addition, during the inspection following FGF-2 administration (Fig. 1), no FGF-2 or anti-FGF-2 antibodies were detected in the serum of any patients.

Discussion

Originally isolated from bovine hypophysis in the 1970s, FGF-2 is a protein with a molecular weight of 17,000 that acts to promote proliferation of fibroblasts. Researchers have isolated, refined and

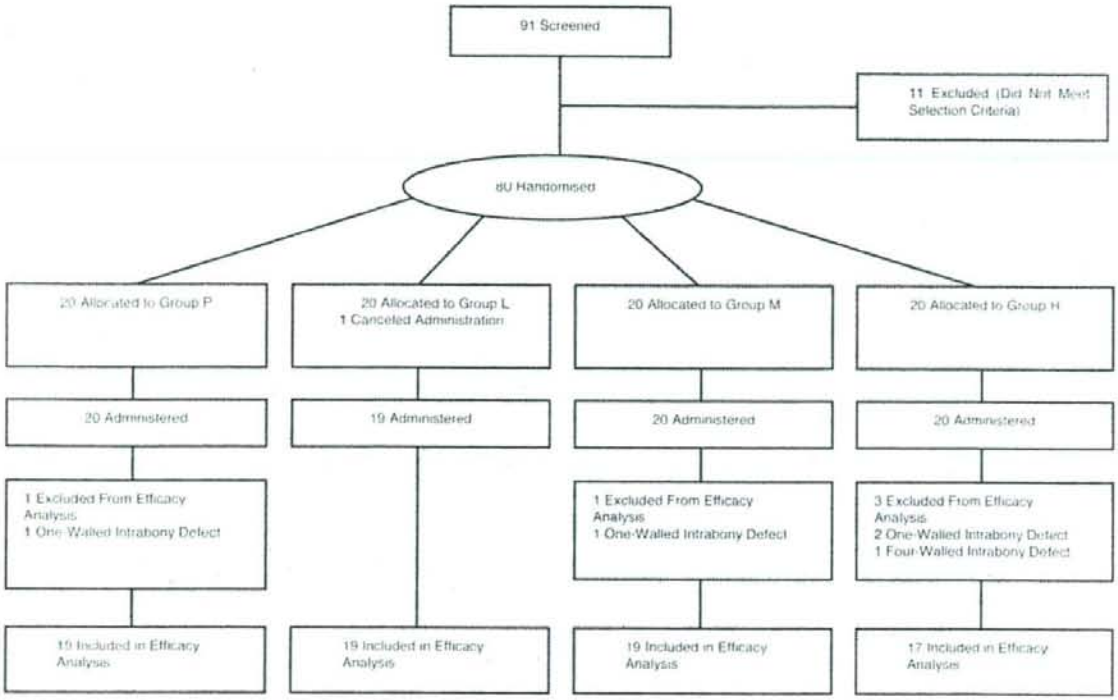

Figure 3. Flow of patients through the study.
doi:10.1371/journal.pone.0002611.g003

genetically cloned human FGF-2 to clarify numerous different biological activities of the protein. As yet, many studies have reported that FGF-2 stimulates proliferation of numerous kinds of cells, including not just fibroblasts, but also vascular endothelial, vascular smooth muscle, neuroectodermal, osteoblast, cartilage and epidermal cells. The protein is now known to be deeply involved in cell proliferation and differentiation and also in control of extracellular matrix generation during the processes of tissue generation and wound healing [20–25]. Many recent reports in the field of regenerative medicine have described the use of cytokines as "signaling molecules", stimulating adequate proliferation and differentiation of tissue stem cells. Among those cytokines, FGF-2 is winning attention from researchers due to activity in promoting proliferation of mesenchymal stem cells while maintaining multilineage potential [6]. The protein has already been utilized in a human intractable ulcer-curing drug (Fiblast Spray; Kaken Pharmaceutical Co., Ltd.) for more than 4 years.

We have already studied the stimulation of periodontal tissue regeneration by FGF-2 in animal models and believe that the protein represents a major candidate for a periodontal tissue-regenerating agent. This is based on stimulation of proliferation for both kinds of cell groups that rebuild hard and soft tissues along with strong angiogenic activity, which is indispensable in tissue regeneration. Animal tests have revealed that in artificial models of periodontal tissue defect in beagles [13,15] and non-human primates (*M. fascicularis*) [14], FGF-2 significantly stimulates neogenesis of alveolar bone, periodontal ligament and cementum, without invoking abnormal effects such as down-growth of the gingival epithelia, resorption of the dental root or ankylosis.

Based on effective concentrations of FGF-2 for periodontal tissue regeneration in animal trials, in addition to the results of our Phase I trial in which FGF-2 was administered intravenously to healthy adult humans, we determined the concentrations and doses administered to periodontal regions of patients in the present clinical trial. More specifically, the results of testing with artificial defect models of periodontal tissue in beagles led us to estimate that an effective FGF-2 concentration for stimulation of periodontal tissue regeneration was 0.03–0.3%. This range of concentrations was therefore applied in the present clinical trial. We selected 200 μL as the dose, considering that this was good enough to work on the defect region of periodontal tissue. In addition, preclinical trial results have suggested that the maximum quantity of administered FGF-2 to enter the circulation in the present trial herein would be around 1.2 mg/body, less than the 30 mg/body for which safety was confirmed in our Phase I trial. The 91 patients screened as subjects and a final total of 80 patients were enrolled as subjects. The patient characteristics were almost similar among groups. However, we understand that we could not perfectly eliminate biasing influences of patient characteristics in this study and a larger scale trial is needed in the future.

In evaluating efficacy, we surveyed 74 cases of 2- or 3-walled intrabony defect that satisfied the selection criteria. To evaluate periodontal tissue regeneration, evaluating fibrous attachment accompanied by neogenesis of alveolar bone and cementum is important. Rate of increase in alveolar bone height observed in close proximity to the dental root was measured as a prespecified primary outcome in this clinical trial.

Use of 0.3% FGF-2 stimulated 58.6% regeneration, which was at least comparable with the previous results within 9 months after

Table 5. Patient characteristics

Item	Classification	Group P	Group L	Group M	Group H
Numbers of patients		20	19	20	20
Sex (% of patients)	Male	55.0	36.8	25.0	35.0
	Female	45.0	63.2	75.0	65.0
Age (years)	Mean (SD)	49.2 (8.9)	46.2 (11.1)	46.8 (10.3)	47.7 (10.5)
Coexisting disease (% of patients)	No	70.0	57.9	75.0	85.0
	Yes	30.0	42.1	25.0	15.0
Previous history	No	75.0	73.7	60.0	60.0
	Yes	25.0	26.3	40.0	40.0
Smoking habit	No	75.0	89.5	80.0	70.0
	Yes	25.0	10.5	20.0	30.0
Region of administration (Major classification) (% of patients)	Maxilla	40.0	57.9	55.0	60.0
	Mandible	60.0	42.1	45.0	40.0
Region of administration (Minor classification) (% of patients)	Anterior tooth	25.0	21.1	25.0	30.0
	Premolar	35.0	42.1	40.0	40.0
	Molar	40.0	36.8	35.0	30.0
Depth of bone defect at operation (mm)	Mean (SD)	4.7 (1.5)	4.8 (2.4)	4.6 (1.7)	5.7 (2.6)
Classification of bone defect (% of patients)	1-walled	5.0	0.0	5.0	10.0
	2-walled	50.0	47.4	70.0	50.0
	3-walled	40.0	47.4	25.0	30.0
	4-walled	0.0	0.0	0.0	5.0
	2/3-walled	0.0	5.3	0.0	5.0
	1/2-walled	5.0	0.0	0.0	0.0
Treatment to tooth of investigation (% of patients)	No	60.0	57.9	55.0	55.0
	Yes	40.0	42.1	45.0	45.0
Existent of dental pulp (% of patients)	No	15.0	15.8	20.0	25.0
	Yes	85.0	84.2	80.0	75.0
Clinical attachment level (mm)	Mean (SD)	9.3 (2.2)	8.4 (2.7)	8.4 (2.8)	8.3 (3.0)
Probing depth (mm)	Mean (SD)	5.7 (1.2)	5.4 (1.6)	5.1 (2.0)	5.8 (1.7)
Recession (mm)	Mean (SD)	2.4 (1.8)	2.1 (1.5)	2.2 (2.3)	1.7 (1.5)
Width of keratinized gingival (mm)	Mean (SD)	4.9 (2.1)	4.3 (1.9)	4.5 (2.2)	5.3 (2.7)
Gingival bleeding index (% of patients)	−	10.0	15.8	20.0	5.0
	+	90.0	84.2	80.0	95.0
Gingival index (% of patients)	0	35.0	21.1	25.0	10.0
	1	30.0	47.4	40.0	45.0
	2	35.0	31.6	35.0	45.0
Mobility of tooth (% of patients)	0	65.0	57.9	50.0	40.0
	1	35.0	36.8	50.0	55.0
	2	0.0	5.3	0.0	5.0
Plaque index (% of patients)	0	50.0	42.1	80.0	60.0
	1	35.0	57.9	20.0	30.0
	2	15.0	0.0	0.0	10.0

doi:10.1371/journal.pone.0002611.t005

regenerative therapy [19,26,27]. However, no significant difference was identified between Groups P and H in terms of millimeter increments ($p = 0.132$). To confirm the efficacy of the investigational drug using more conventional methods, data in both % and millimeter increments were used to calculate sample size for the next late Phase II trial. In addition, the minimum clinically effective dose will need to be assessed and determined in a future clinical study involving more patients.

Interestingly, no significant difference was observed between the 4 groups in the millimeter of CAL regained, with all groups scoring around 2 mm (see Table S2 of supporting items). The CAL regained following periodontal surgery is derived from the sum of epithelial and fibrous attachments. If periodontal tissue regeneration accompanied by neogenesis of the alveolar bone and cementum is stimulated, fibrous attachment reproducing the natural anatomical morphology is achieved. However, the

Table 6. Changes with time in alveolar bone height

		Group P (n = 19)	Group L (n = 19)	Group M (n = 19)	Group H (n = 17)
rate of increase (%)	12 weeks	6.90 (20.12)	2.03 (18.79)	−0.82 (33.1)	13.86 (33.03)
	24 weeks	17.44 (28.48)	12.33 (27.50)	12.59 (23.67)	35.58 (40.35)
	36 weeks	23.92 (27.52)	20.19 (38.09)	29.39 (37.71)	*58.62 (46.74)
millimeter increase	12 weeks	0.28 (0.80)	0.07 (0.58)	0.15 (0.71)	0.55 (1.37)
	24 weeks	0.67 (1.25)	0.38 (0.97)	0.53 (0.71)	1.21 (1.57)
	36 weeks	0.95 (1.26)	0.54 (1.26)	1.06 (1.16)	1.85 (1.75)

Mean and standard deviations are shown. *A significant difference (p = 0.021) was only identified between Group P and Group H at 36 weeks in rate of increase in alveolar bone height.

doi:10.1371/journal.pone.0002611.t006

majority of CAL acquisition following conventional periodontal surgery has been shown to be due to epithelial attachment unaccompanied by alveolar bone regeneration [28–31]. We have previously conducted an animal study using non-human primates and reported that at the FGF-2 administration site, down-growth of gingival epithelial cells was suppressed to achieve fibrous attachment accompanied by neogenesis of the alveolar bone and cementum [14]. In the present study, no significant differences in CAL regained were seen between Group P (conventional periodontal surgery) and the three FGF-2 groups (Table 8). Based on the results of the above-mentioned preclinical study, we deduce that differences may exist between Group P and the three FGF-2 groups in histological ratio of fibrous and epithelial attachments achieving CAL acquisition. Confirmation of the nature of healing tissue requires histological evaluation in a future study.

PD, BOP, GI, MO, REC and KG are generally used to assess pathology in periodontal disease. These parameters do not directly assess the efficacy of FGF-2 in periodontal tissue regeneration, and were selected in the present study as secondary outcome measures to ascertain whether FGF-2 would cause abnormal periodontal healing following periodontal surgery. The fact that no significant differences among these secondary outcome measures for the 4 groups showed that FGF-2 administration did not cause abnormal healing of periodontium following periodontal surgery. Furthermore, frequency of PD, GI, and BOP all dropped over time in all groups after periodontal surgical treatment. These findings show that we can expect FGF-2 administration to provide a therapeutic process similar to that of the conventional flap operation, in addition to the healing outcome of periodontal tissue regeneration. Yet another observation was the lack of recognisable difference in changes to REC and KG, which accompanies periodontal surgical treatment, between Group P and the other 3 groups receiving FGF-2 administration. This confirms that FGF-2 administration does not cause peculiar gingival recession or reduce keratinized gingiva. PII offers a parameter for assessing the amount of plaque causing periodontal disease, and since the degree of plaque deposition can affect the prognosis of periodontal surgery, this parameter was also selected as a secondary outcome measure. In this clinical study, no significant intergroup differences were seen in PII. Moreover, radiography was performed for 67 patients who willingly and positively responded to our "recall" for imaging between week 83 and 132 (inclusive) after administration of investigational drugs (Group P, n = 19; Group L, n = 15; Group M, n = 18; Group H, n = 16). Among these 67 patients, no cases suggested an abnormal increase in alveolar bone exceeding the cementoenamel junction or an equivalent control point or ankylosis (data not shown).

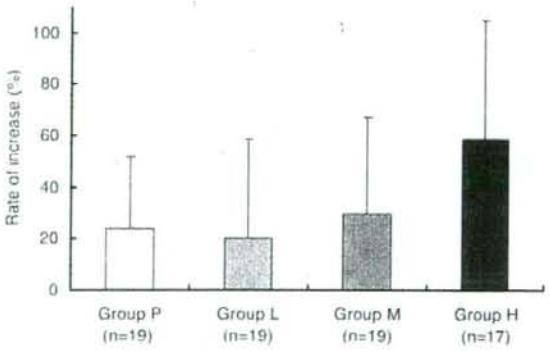

Figure 4. Rates of increase in alveolar bone height in cases of 2- and 3-walled intrabony defects. We compared rates of increase in alveolar bone height at 36 weeks after FGF-2 administration among Group P (19 placebo cases), Group L (19 cases administered 0.03% FGF-2), Group M (19 cases administered 0.1% FGF-2) and Group H (17 cases administered 0.3% FGF-2). This figure shows mean increase rates (%) and standard deviations of alveolar bone height. While no significant difference was observed between Groups L and M and P, Group H showed significantly increased (p = 0.021) alveolar bone height in the bone defect region compared to Group P.

doi:10.1371/journal.pone.0002611.g004

The periodontal ligament comprises heterogenous cell populations and researchers have predicted the existence of some progenitor cells that can differentiate into cementoblasts or osteoblasts [32–34]. A recent study reported that some cells within the ligament express STRO-1 and CD146 mesenchymal stem cell markers. Such cells, according to the study, differentiate into cementoblast-like cells, adipocytes and collagen-forming cells. Our previous in vitro studies have clarified that FGF-2 facilitates proliferation while maintaining the differentiation of human periodontal ligament cells (HPDLs). In addition, we now know that the protein does not just stimulate angiogenesis, an action indispensable in the regeneration of tissue, but also increases the production of various types of extracellular matrix from HPDLs [21,35–37]. In short, FGF-2 creates a local environment suitable for the regeneration of periodontal tissue through the activities described above, as part of the mechanism by which regeneration of periodontal tissue is stimulated.

In our clinical trial, to identify adverse events from FGF-2 administered to a particular region of periodontal tissue, we conducted an interview and visual inspection to check the whole body of the patient, checked oral cavity findings and performed clinical inspection. No relationships were identified between

Table 7. Changes in alveolar bone height at 36 weeks

		Group P (n = 19)	Group L (n = 19)	Group M (n = 19)	Group H (n = 17)
rate of increase (%)	Mean (SD)	23.92 (27.52)	20.19 (38.09)	29.39 (37.71)	58.62 (46.74)
	Mean differences		−3.73	5.47	34.7
	from Group P (95%CI)		(−28.22–20.77)	(−19.02–29.97)	(9.50–59.91)
	Adjusted p value*		0.981	0.945	0.021
millimeter increase	Mean (SD)	0.95 (1.26)	0.54 (1.26)	1.06 (1.16)	1.85 (1.75)
	Mean differences		−0.41	0.11	0.90
	from Group P (95%CI)		(−1.24–0.42)	(−0.69–0.91)	(−0.13–1.92)
	Adjusted p value*		0.678	0.990	0.132

*Adjusted for multiple comparisons based on Dunnett's test.
doi:10.1371/journal.pone.0002611.t007

administration of the investigational drug and the frequency of any adverse events (see Table S4 of supporting items). Although some adverse events did emerge in patients administered FGF-2, no relationship was recognizable between frequency of these events and FGF-2 concentrations. In addition, the same adverse events also emerged in the placebo group. Those effects are therefore not specific to groups administered FGF-2 and do not appear attributable to the drugs administered. Another reason why we consider that FGF-2 administered locally to periodontal tissue seldom travels through the whole body to create adverse drug reactions is that the protein was undetectable in serum after drug administration. Furthermore, no patients displayed increased levels of anti-FGF-2 antibody after administration, suggesting that FGF-2 is free from antibody production, an adverse drug reaction often seen with other proteinaceous agents. In short, none of the results of this particular clinical trial suggest any clinical problems concerning the safety of administering FGF-2 to patients with periodontitis. One more piece of evidence supporting the high safety of FGF-2 applied locally to periodontal tissue is that this therapy has already been used for more than 5 years as a remedy for intractable ulcers (Fiblast spray).

Periodontitis shortens the life of teeth and can thus reduce QOL in middle-aged to elderly individuals [4]. To maintain and promote oral health, new therapies must be established for safe and efficient regeneration of periodontal tissue. Cytokine therapy has thus been winning attention for the last decade [6–15,19]. However, few double-blinded clinical trials have used multiple facilities in compliance with GCP guidelines to confirm the efficacy of a single cytokine alone as a stimulator of periodontal tissue regeneration. In the present clinical trial, 0.3% FGF-2 improved CAL by about 2 mm at 36 weeks from base. And more importantly, rate of increase in bone height observed in close proximity to the dental root was significantly improved in 0.3% FGF-2 treatment group compared to placebo group at 36 weeks. These findings were clinically interpreted that some efficacy could be expected from FGF-2 in stimulating regeneration of periodontal tissue. Thus, we concluded in this study that FGF-2 therapy can be efficacious in regenerating periodontal tissue. However, an important limitation of this study is the small sample size of the trial. This trial is still preliminary, and several trials need to be performed before FGF-2 drug can be placed on the market. In future, we plan to clarify the efficacy of FGF-2 drug, determine the optimal dose for clinical use and confirm in more detail the safety of FGF-2 in a large Phase II study. And then Phase III will be performed to confirm the efficacy and safety of the invitational drug.

(This clinical trial was conducted at the request of Kaken Pharmaceutical Co., Ltd.)

Supporting Information

Checklist S1 CONSORT Checklist.
Found at: doi:10.1371/journal.pone.0002611.s001 (0.04 MB DOC)

Protocol S1 Trial Protocol.
Found at: doi:10.1371/journal.pone.0002611.s002 (0.11 MB DOC)

Table 8. Clinical Attachment Level (CAL) regained at 36 weeks

		Group P (n = 19)	Group L (n = 19)	Group M (n = 19)	Group H (n = 17)
mm of CAL regained	Mean (SD)	2.63 (1.54)	2.00 (2.08)	2.02 (2.08)	2.18 (1.33)
	Mean differences		−0.63	−0.61	−0.46
	From Group P (95%CI)		(−1.84–0.57)	(−1.81–0.60)	(−1.43–0.53)
	Adjusted p value*		0.573	0.604	0.792
% of CAL regained	Mean (SD)	29.65 (17.00)	24.03 (25.31)	24.20 (28.27)	29.69 (23.14)
	Mean differences		−5.62	−5.45	0.04
	from Group P (95%CI)		(−19.81–8.60)	(−20.79–9.90)	(−13.61–13.70)
	Adjusted p value*		0.810	0.823	1.000

*Adjusted for multiple comparisons based on Dunnett's test.
doi:10.1371/journal.pone.0002611.t008

Table S1 Clinical inspections.
Found at: doi:10.1371/journal.pone.0002611.s003 (0.03 MB DOC)

Table S2 Changes in periodontal tissue. Mean and standard deviations are shown. *Data at 36 weeks were missing for 1 patient in Group M.
Found at: doi:10.1371/journal.pone.0002611.s004 (0.07 MB DOC)

Table S3 Changes in periodontal tissue. All of data at 36 weeks were missing for 1 patient in Group M. Data for MO were missing at 12 weeks for each patient in Groups P and H, at 24 weeks in Group H and at 36 weeks in Group H.
Found at: doi:10.1371/journal.pone.0002611.s005 (0.07 MB DOC)

Table S4 List of adverse drug reactions. *Pains experienced by 1 patient in Group M required therapy, and the patient began to experience pain at the surgical site starting 8 days after administration that resolved 35 days after administration with the use of drugs such as cefcapene pivoxil hydrochloride, lysozyme hydrochloride, rebamipide and loxoprofen sodium.

Found at: doi:10.1371/journal.pone.0002611.s006 (0.04 MB DOC)

Acknowledgments

We wish to thank all the investigators who participated and most of all the patients for their important contributions to the study. We would also like to thank Katsuyasu Eguchi, Toshiyuki Yorozuya, Hayuru Koizumi, Shinya Horimoto, Motoki Akamatsu (Kaken Pharmaceutical Co., Ltd.) and Takenori Nozaki (Osaka University Dental Hospital) for their critical support of this study.

Author Contributions

Conceived and designed the experiments: SM MK MW. Performed the experiments: MK KN YK TF HS MF TN TS YI ST HK MN JK TN TH KM YH YI TH. Analyzed the data: SM MK MW. Wrote the paper: SM MK KN TF HS MF TN TS YI ST HK MN JK TN TH KM YH YI TH MW. Other: Measured the X-ray film data: TF TS. Participated in interpretation of the results: TF EI MO TS. Confirmed safety of all patients throughout the study period: MO EI.

References

1. Nishihara T, Koseki T (2004) Microbial etiology of periodontitis. Periodontology 2000 36: 14–26.
2. Socransky SS, Haffajee AD (2002) Dental biofilms: difficult therapeutic targets. Periodontology 2000 28(1): 12–55.
3. Ezzo PJ, Cutler CW (2003) Microorganisms as risk indicators for periodontal disease. Periodontology 2000 32(1): 24–35.
4. Kinane DF (2001) Causation and pathogenesis of periodontal disease. Periodontology 2000 25(1): 8–20.
5. Seo BM, Miura M, Gronthos S, Bartold PM, Batouli S, et al. (2004) Investigation of multipotent postnatal stem cells from human periodontal ligament. Lancet 364: 149–155.
6. Lynch SE, Williams RC, Polson AM, Howell TH, Reddy MS, et al. (1989) A combination of platelet-derived and insulin-like growth factors enhances periodontal regeneration. J Clin Periodontol 16: 545–548.
7. Kinoshita A, Oda S, Takahashi K, Yokota S, Ishikawa I (1997) Periodontal regeneration by application of recombinant human bone morphogenetic protein-2 to horizontal circumferential defects created by experimental periodontitis in beagle dogs. J Periodontol 68: 103–109.
8. Sigurdsson TJ, Lee MB, Kubota K, Turek TJ, Wozney JM, et al. (1995) Periodontal repair in dogs: recombinant human bone morphogenetic protein-2 significantly enhances periodontal regeneration. J Periodontol 66: 131–138.
9. Mohammed S, Pack AR, Kardos TB (1998) The effect of transforming growth factor beta one (TGF-beta 1) on wound healing, with or without barrier membranes, in a Class II furcation defect in sheep. J Periodontal Res 33: 335–344.
10. Giannobile WV, Ryan S, Shih MS, Su DL, Kaplan PL, et al. (1998) Recombinant human osteogenic protein-1 (OP-1) stimulates periodontal wound healing in class III furcation defects. J Periodontol 69: 129–137.
11. Takeda K, Shiba H, Mizuno N, Hasegawa N, Mouri Y, et al. (2005) Brain-derived neurotrophic factor enhances periodontal tissue regeneration. Tissue Eng 11: 1618–1629.
12. Nevins M, Giannobile WV, McGuire MK, Kao RT, Mellonig JT, et al. (2005) Platelet-derived growth factor stimulates bone fill and rate of attachment level gain: results of a large multicenter randomized controlled trial. J Periodontol 76: 2205–2215.
13. Murakami S, Takayama S, Ikezawa K, Shimabukuro Y, Kitamura M, et al. (1999) Regeneration of periodontal tissues by basic fibroblast growth factor. J Periodont Res 34: 425–430.
14. Takayama S, Murakami S, Shimabukuro Y, Kitamura M, Okada H (2001) Periodontal regeneration by FGF-2 (bFGF) in primate models. J Dent Res 80: 2075–2079.
15. Murakami S, Takayama S, Kitamura M, Shimabukuro Y, Yanagi K, et al. (2003) Recombinant human basic fibroblast growth factor (bFGF) stimulates periodontal regeneration in class II furcation defects created in beagle dogs. J Periodont Res 38: 97–103.
16. Löe H, Silness J (1963) Periodontal disease in pregnancy. I. Prevalence and severity. Acta Odontol Scand 21: 533–551.
17. Miller SC (1950) Textbook of Periodontia, 3rd ed. Philadelphia and Toronto: The Blakiston Co.
18. Silness J, Löe H (1964) Periodontal disease in pregnancy. II. Correlation between oral hygiene and periodontal condition. Acta Odontol Scand 22: 121–135.
19. Howell TH, Fiorellini JP, Paquette DW, Offenbacher S, Giannobile WV, et al. (1997) A phase I/II clinical trial to evaluate a combination of recombinant human platelet-derived growth factor-BB and recombinant human insulin-like growth factor-I in patients with periodontal disease. J Periodontol 68: 1186–1193.
20. Ledoux D, Gannoun-Zaki L, Barritault D (1991) Interactions of FGFs with target cells. Prog Growth Factor Res 4: 107–120.
21. Takayama S, Yoshida J, Hirano H, Okada H, Murakami S (1997) Effects of basic fibroblast growth factor on human gingival epithelial cells. J Periodont Res 32: 667–675.
22. Gibran NS, Isik FF, Heimbach DM, Gordon D (1994) Basic fibroblast growth factor in the early human burn wound. J Surg Res 56: 226–234.
23. Yu W, Naim JO, Lanzafame RJ (1994) Expression of growth factors in early wound healing in rat skin. Lasers Surg Med 15: 281–289.
24. Richard JL, Parer-Richard C, Daures JP, Clouet S, Vannereau D, et al. (1995) Effect of topical basic fibroblast growth factor on the healing of chronic diabetic neuropathic ulcer of the foot. A pilot, randomized, double-blind, placebo-controlled study. Diabetes Care 18: 64–69.
25. Okumura M, Okuda T, Nakamura T, Yajima M (1996) Acceleration of wound healing in diabetic mice by basic fibroblast growth factor. Biol Pharm Bull 19: 530–535.
26. Kilic AR, Efeoglu E, Yilmaz S (1997) Guided tissue regeneration in conjunction with hydroxyapatite-collagen grafts for intrabony defects. A clinical and radiological evaluation. J Clin Periodontol 24: 372–383.
27. Zetterstrom O, Andersson C, Eriksson L, Fredriksson A, Friskopp J, et al. (1997) Clinical safety of enamel matrix derivative (EMDOGAIN) in the treatment of periodontal defects. J Clin Periodontol 24: 697–704.
28. Egelberg J (1987) Regeneration and repair of periodontal tissues. J Periodont Res 22: 233–242.
29. Caton J, Zander HA (1976) Osseous repair of an infrabony pocket without new attachment of connective tissue. J Clin Periodontol 3: 54–58.
30. Wikesjo UM, Nilveus R (1991) Periodontal repair in dogs. Healing patterns in large circumferential periodontal defects. J Clin Periodontol 18: 49–59.
31. Bowers GM, Schallhorn RG, Mellonig JT (1982) Histologic evaluation of new attachment in human intrabony defects. A literature review. J Periodontol 53: 509–514.
32. Shimono M, Ishikawa T, Ishikawa H, Matsuzaki H, Hashimoto S, et al. (2003) Regulatory mechanisms of periodontal regeneration. Microsc Res Tech 60: 491–502.
33. Lekic P, Rojas J, Birek C, Tenenbaum H, McCulloch CA (2001) Phenotypic comparison of periodontal ligament cells in vivo and in vitro. J Periodont Res 36(2): 71–79.
34. Murakami Y, Kojima T, Nagasawa T, Kobayashi H, Ishikawa I (2003) Novel isolation of alkaline phosphatase-positive subpopulation from periodontal ligament fibroblasts. J Periodontol 74(6): 780–786.
35. Shimabukuro Y, Ichikawa T, Takayama S, Yamada S, Takedachi M, et al. (2005) Fibroblast growth factor-2 regulates the synthesis of hyaluronan by human periodontal ligament cells. Matrix Biol. In press.
36. Shimabukuro Y, Ichikawa T, Terashima Y, Iwayama T, Oohara H, et al. (2008) Basic fibroblast growth factor regulates expression of heparan sulfate in human periodontal ligament cells. Matrix Biol. In press.
37. Terashima Y, Shimabukuro Y, Terakura M, Ikezawa K, Hashikawa T, et al. (2008) Fibroblast growth factor-2 regulates expression of osteopontin in periodontal ligament cells. J Cell Physiol. In press.

Biochemical and Biophysical Research Communications 371 (2008) 191–196

Contents lists available at ScienceDirect

Biochemical and Biophysical Research Communications

journal homepage: www.elsevier.com/locate/ybbrc

PLAP-1/asporin inhibits activation of BMP receptor via its leucine-rich repeat motif

M. Tomoeda [a], S. Yamada [a], H. Shirai [b], Y. Ozawa [a], M. Yanagita [a], S. Murakami [a,*]

[a] Department of Periodontology, Division of Oral Biology and Disease Control, Osaka University Graduate School of Dentistry, 1-8 Yamadaoka, Suita, Osaka 565-0871, Japan
[b] Advanced Genomics, Molecular Medicine Laboratories, Astellas Pharma, 21 Miyukigaoka Tsukuba-city, Ibaraki 305-8585, Japan

ARTICLE INFO

Article history:
Received 24 March 2008
Available online 11 April 2008

Keywords:
PLAP-1
Asporin
SLRP
BMP-2
Smad
Leucine-rich repeat

ABSTRACT

We previously identified the novel gene, periodontal ligament-associated protein-1 (PLAP-1)/asporin and reported that PLAP-1/asporin inhibited bone morphogenetic protein-2 (BMP-2)-induced cytodifferentiation of periodontal ligament (PDL) cells probably by direct interaction with BMP-2. Here, we elucidated the detailed regulatory mechanism of this protein on BMP-2-induced cytodifferentiation of PDL cells. Recombinant PLAP-1/asporin inhibited BMP-2-induced cytodifferentiation of PDL cells and competitively prevented BMP-2 from binding to the BMP receptor-IB (BMPR-IB), resulting in inhibition of BMP-dependent activation of Smad proteins. The induction of mutation to the leucine-rich repeat (LRR) motif, especially LRR5, within PLAP-1/asporin rescued the inhibitory effect of PLAP-1/asporin on BMP-2. By contrast, a 26-amino acid peptide in the PLAP-1/asporin LRR5 sequence inhibited BMP-2 activity. Our findings indicate that PLAP-1/asporin inhibits BMP-2-induced differentiation of PDL cells resulting from inactivation of the BMP-2 signaling pathway and that LRR, especially LRR5 of PLAP-1/asporin, plays an important role in the PLAP-1/asporin–BMP-2 interaction.

The periodontal ligament (PDL) is a connective tissue that surrounds the roots of the tooth and attaches the roots to the alveolar bone to mechanically support teeth and to play nutritive and sensory roles [1]. Moreover, the PDL plays an important role as a reservoir of multipotential mesenchymal stem cells that can differentiate into mineralized tissue-forming cells such as osteoblasts and cementoblasts [2,3]. The PDL constitutively expresses mRNA of alkaline phosphatase (ALPase), type I collagen, periostin and Runx-2 [4], suggesting that the PDL possesses a strong potential for hard-tissue formation. However, the PDL tissue is never ossified *in vivo*. This indicates that inhibitory mechanisms for matrix mineralization constantly exist within the PDL.

In order to clarify the uniqueness of the PDL at the molecular level, we previously examined the gene expression profile and identified a novel gene, PLAP-1, which belongs to the small leucine-rich proteoglycan (SLRP) family class I [5]. Interestingly, we found that PLAP-1/asporin inhibited bone morphogenetic protein-2 (BMP-2)-induced cell differentiation probably by binding to BMP-2 directly [6].

In addition to the tissue-specific expression of BMP-2 and cell surface receptors, BMP-2 signaling is precisely regulated by certain classes of molecules. Some SLRP family proteins were reported to directly associate with transforming growth factor-beta (TGF-β) and BMP-4 and served as their antagonists/agonists appropriate to the circumstances [7–9].

The LRR motif is very widely distributed and has been found in more than 100 intracellular and extracellular proteins. This motif is well conserved from humans to insects, associates with metal ions, DNA, other proteins, and exerts a variety of functions [10]. Interestingly, previous reports showed that a high affinity binding site for decorin and TGF-β is located between LRR3-5 of the decorin core protein [11], and that decorin binds to collagen mainly through its LRR4-5 [12].

Based on these reports and structural characteristics, we elucidated the PLAP-1/asporin regulatory mechanism in detail on BMP-2-induced cytodifferentiation of PDL cells.

Materials and methods

Cell culture. We have established a mouse PDL cloned cell line, MPDL22, and maintained MPDL22 cells as previously described [6].

Generation of recombinant PLAP-1/asporin protein. Recombinant mouse PLAP-1/asporin protein was generated from *Escherichia coli*. Mouse PLAP-1/asporin cDNA expressing pET29b vector was gifted by Dr. Ikegawa, RIKEN (Tokyo, Japan). We expressed and extracted protein as previously described [13] and removed the LPS using the Detoxi-Gel Endotoxin Removing Gel (PIERCE, Rockford, IL, USA).

Alkaline phosphatase activity and cellular DNA content. ALPase activity was assessed according to the procedure of Bessay et al. and DNA content was measured using a modification of the method of Labarca and Pagien as previously described [6].

* Corresponding author. Fax: +81 6 6879 2934.
E-mail address: ipshinya@dent.osaka-u.ac.jp (S. Murakami).

0006-291X/$ - see front matter © 2008 Elsevier Inc. All rights reserved.
doi:10.1016/j.bbrc.2008.03.158

Real-time PCR analysis. The total RNA was extracted from MPDL22 cells using the RNA easy kit (Qiagen, Germantown, MD, USA) according to the manufacturer's protocol. About 0.4 μg of total RNA extract was reverse-transcribed with the High Capacity cDNA Reverse Transcriptase kit (Applied Biosystems, Foster-city, CA, USA) to generate the single-stranded cDNA. PCR reactions were carried out using the ABI 7300 Fast Real-Time PCR System (Applied Biosystems) with the Power SYBR® Green PCR Master Mix (Applied Biosystems) according to the manufacturer's protocol. All reactions were run in triplicate. The primer sequences are available upon request.

Competitive sequential immunoprecipitation assay for BMP-2 binding to the BMP receptor and Western blotting. We incubated 0.6 μg recombinant mouse BMPR-IB/ALK6/Fc chimera (R&D Systems, Inc., Minneapolis, MN, USA) with the Protein G sepharose (Amersham) in a rotator at 4 °C for 1 h. At the same time, we incubated 0.6 μg recombinant human BMP-2 and various doses of recombinant PLAP-1/asporin protein. Then we mixed them and incubated at 4 °C for 1 h. We collected the immunoprecipitated complex by centrifugation. This was then separated by SDS–PAGE and blotted onto PVDF membranes. As a primary antibody, we used rabbit anti-BMPR-IB antibody (H-44) (1:250; Santa Cruz Biotech, Santa Cruz, CA, USA) and streptavidin-conjugated goat anti-BMP-2/4 antibody (1:250; R&D Systems). As a secondary antibody, we used horseradish peroxidase-linked goat anti-rabbit IgG antibody (Cappel, Aurora, OH, USA) and horseradish peroxidase-linked anti-streptavidin antibody (Amersham). We detected immunoreactive proteins using the ECL plus kit (Amersham).

Western blotting for BMP-dependent Smad-1/5/8. MPDL22 cells treated with BMP-2 in the presence or absence of recombinant PLAP-1/asporin protein for 30 min were washed twice with ice-cold PBS, and lysed with the lysis buffer (50 mM Tris-HCl (pH 7.4), 1% NP-40, 0.25% sodium deoxycholate, 150 mM NaCl, 1 mM EDTA, 1 mM Na_3VO_4, 1 mM NaF, and a tablet of Complete Mini (Roche Diagnostic GmbH, Penzberg, Germany) per 10 ml). The protein concentrations of the cell lysates were measured using the BCA protein assay kit (PIERCE, Rockford, IL, USA) according to the manufacturer's instructions. As a primary antibody, we used mouse anti-Smad1 antibody (1:100; Santa Cruz Biotech) and rabbit anti-phospho-Smad1/5/8 antibody (1:500; Cell Signaling Technology, Beverly, MA, USA). As a secondary antibody, we used horseradish peroxidase-linked goat anti-mouse IgG antibody (Santa Cruz Biotech) and horseradish peroxidase-linked goat anti-rabbit IgG antibody (Cappel).

Building of the tertiary structural model of mouse PLAP-1/asporin. The tertiary structural model of mouse PLAP-1/asporin was built by the homology modeling technique. We chose the complex structure of bovine biglycan dimer (PDB Code 2FT3 [14]) as the template because the protein is the closest homologue of PLAP-1/asporin whose 3D-structure has been determined by X-ray crystallography. The alignment of PLAP-1/asporin and biglycan was carried out by the software Clustal W [15], and then a total of ten models were constructed by the software MOE (*Molecular Operating Environment*, version 2006.0801; Chemical Computing Group Inc., Montreal, Que., Canada.) We used the software JOY [16] to evaluate the models, and chose the best model for the inspection. The precise inspection was carried out by software MOE and Rasmol [17].

Generation of stable PLAP-1/asporin mutant overexpressing cell clones. PLAP-1/asporin/3XFLAG expression vector was prepared as previously described [6]. The plasmids harboring the cDNA for PLAP-1/asporin mutants, I (E194K), II (E194G), and III (R170E, R219E) were generated from the respective wild-type plasmid, PLAP-1/asporin/3XFLAG expression vector, by the Quick Change Site-Directed Mutagenesis kit (Stratagene, LA Jolla, CA, USA) in accordance with the manufacturer's protocol using the following primer pairs: forward, 5′-GCTTTACATGTTTTGAAAATGAGTGCAAACCCTC-3′ and reverse, 5′-GAGGGTTTGCACTCATTTTCAAAACATG TAAAGC-3′ for E194K; forward, 5′-GCTTTACATGTTTTGGGAATGAGTGCAAACCCTC-3′ and reverse, 5′-GAGGGTTTGCACTCATTCCCAAAACATGTAAAGC-3′ for E194G; forward, 5′-CCCAAATCATTAGCAGAACTCGAAATTCATGATAATAAAG-3′ and reverse, 5′-CTTTATTATCATCATGAATTTCGAGTTCTGCTAATGATTTGGG-3′ for R170E; forward, 5′-GGTGACAGTATTCCATATCGAGATCGCTGAAGCAAAAC-3′ and reverse, 5′-GTTTTGCTTCAGCGATCTCGATATGGAATACTGTCACC-3′ for R219E. The sequence was verified by 310 Genetic Analyzer. We plated 5×10^4 of the MPDL22 cells per well in a 6-well plate (Corning Inc., Corning, NY, USA). After 24 h, we transfected the cells with the PLAP-1/asporin/3XFLAG expression vector using Effectene Transfection Reagent (Invitrogen, Carisbad, CA, USA) in accordance with the manufacturer's protocol. The cells were selected for neomycin resistance by adding 400 μg/ml G418 (Invitrogen).

Synthesis of the LRR5/PLAP-1/asporin peptide. We synthesized the 26-residue leucine-rich repeat 5 (LRR5) peptide of mouse PLAP-1/asporin core protein at Thermo Electron GmbH with amino acid sequence of ALHVLEMSANPLENNGIEPGAFEGVT. We used a randomly scrambled sequence for the control peptide: TALEAPVEGPIGFLENNLEVHGSMNA. Amino-ethoxy-ethoxy-acetic acid was conjugated into the N-terminus for improving hydrophilicity.

Statistical analysis. All the experiments in this study were conducted at least three times. We show the representative results. Experimental values were given as means ± SD of triplicate assays. The statistical significance of the differences between two means was examined by the Mann–Whitney *U* test; *P* values less than 0.05 were considered to indicate a significant difference.

Results

PLAP-1/asporin inhibits BMP-2-induced cytodifferentiation

In our previous study, we showed that overexpression of PLAP-1/asporin inhibited BMP-2-induced cytodifferentiation [6]. To investigate the effect of PLAP-1/asporin on BMP-2-induced cytodifferentiation at the protein level, we treated MPDL22 with BMP-2 in the presence or absence of recombinant PLAP-1/asporin protein. N-terminal BAP control protein (SIGMA, St. Louis, MO, USA), which was a non-functional protein, was used as control. When the cells were treated with 0.5 μg and 1 μg recombinant PLAP-1/asporin protein, both BMP-2-induced ALPase activity and osterix mRNA expression were suppressed (Fig. 1A and B).

PLAP-1/asporin inhibits BMP-2 binding to BMPR-IB

We previously showed that PLAP-1/asporin binds to BMP-2 directly [6]. Thus, we speculated that the inhibitory effect of PLAP-1/asporin on BMP-2-induced cytodifferentiation of MPDL22 was caused by the inhibition of BMP-2 binding to the BMP receptor. To clarify this hypothesis, we performed the competitive sequential immunoprecipitation assay. In the presence of BAP control protein, BMP-2 was co-immunoprecipitated with BMPR-IB. However, the addition of recombinant PLAP-1/asporin reduced co-immunoprecipitated BMP-2 in a dose-dependent manner (Fig. 2A).

PLAP-1/asporin inhibits the phosphorylation of BMP-dependent Smad proteins

Since PLAP-1/asporin was revealed to prevent BMP-2 from binding to BMPR-IB, we further examined whether PLAP-1/asporin inhibited the BMP-dependent phosphorylation of Smads1/5/8. Western blotting analysis revealed that total Smad1/5/8 existed consistently and the phosphorylation of these Smads was initiated by BMP-2 stimulation, then after 30 min the phosphorylation reached the maximum level (data not shown). When we stimulated MPDL22 cells with BMP-2 in the presence of PLAP-1/asporin, the phosphorylation of Smad1/5/8 was inhibited (Fig. 2B).

Mutation to LRR5/PLAP-1/asporin rescues the PLAP-1/asporin inhibitory effects on BMP-2-induced cytodifferentiation

Since we revealed that PLAP-1/asporin directly binds to BMP-2, we further investigated the binding site of PLAP-1/asporin. A recent report revealed that decorin mutants, harboring an amino acid substitution of Glu-180 for Lys, showed differential interaction with types I and VI collagen [18]. In order to gain further insight into the molecular structure and function of PLAP-1/asporin, we first built a tertiary structural model of mouse PLAP-1/asporin (Fig. 3A and B). This model demonstrated that negatively charged Glu-194 of mouse PLAP-1/asporin corresponds to Glu-180 of human decorin, situated at the surface, and is sandwiched between positively charged Arg-170 (LRR4) and Arg-219 (LRR6). These ionic residues attracted our attention for their potential involvement in the PLAP-1/asporin–BMP-2 interaction.

Therefore, we induced mutation into these residues. We generated stable clones of MPDL22 cells expressing wild-type PLAP-1/asporin, mutant I (E194K), mutant II (E194G), and mutant III (R170E, R219E) (Fig. 3C). Although the cells expressing wild-type PLAP-1/asporin showed decreased levels of ALPase activity and osterix mRNA expression, the cells expressing mutant I (E194K) and mutant II (E194G) showed almost the same or rather high levels of ALPase activity and osterix mRNA expression compared with those of control cells. On the other hand, the cells expressing mu-

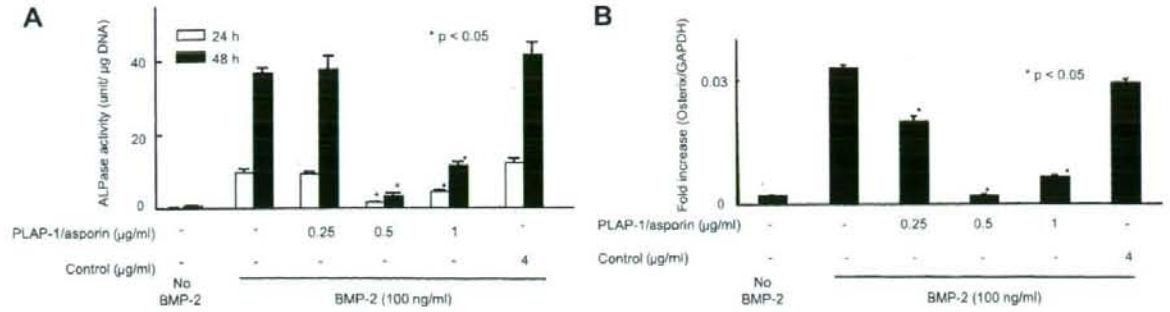

Fig. 1. PLAP-1/asporin inhibits BMP-2-induced cytodifferentiation. (A) ALPase activity in MPDL22 cells cultured for 24 h and 48 h with BMP-2 (100 ng/ml) in the presence or absence of PLAP-1/asporin recombinant protein at the indicated concentrations or N-terminal BAP control protein (4 μg/ml). (B) Real-time PCR analysis of osterix mRNA expression using total RNA isolated from the above-mentioned MPDL22 cells at 48 h treatment. Data represent means ± SEM in triplicate assays. $^{*}P < 0.05$ (Mann–Whitney U test) vs. N-terminal BAP control protein treatment.

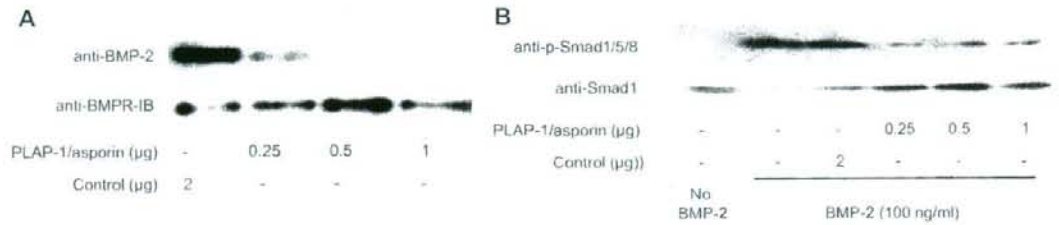

Fig. 2. PLAP-1/asporin inhibits BMP-2 binding to BMPR-IB and the sequential signal transduction. (A) PLAP-1/asporin inhibited BMP-2 binding to BMPR-IB. The competitive inhibition assay was performed. BMPR-IB was incubated with BMP-2 in the presence or absence of recombinant PLAP-1/asporin protein at the indicated concentrations or N-terminal BAP control protein (2 μg). In the presence of N-terminal BAP control protein, BMP-2 (upper panel) was co-immunopreciptated with BMPR-IB (lower panel). The addition of PLAP-1/asporin reduced co-immunoprecipitated BMP-2 in a dose-dependent manner. (B) The effect of PLAP-1/asporin on the BMP-2-induced phosphorylation of Smad1/5/8 determined by Western blot analysis using anti-phospho-Smad1/5/8 antibody (upper panels). Whole cell extracts were lysed from MPDL22 cells after 30 min treatment with BMP-2 (100 ng/ml) in the presence or absence of recombinant PLAP-1/asporin protein at the indicated concentrations or N-terminal BAP control protein (2 μg). The lower panel shows the expression of Smad1 to demonstrate normalized loading of protein.

tant III (R170E, R219E) showed suppression of them, but the level of the suppression was approximately half compared to wild-type PLAP-1/asporin expressing cells (Fig. 3D and E).

LRR5/PLAP-1/asporin peptide inhibits BMP-2-induced cytodifferentiation

To further verify the contribution of LRR5 to the interaction between PLAP-1/asporin and BMP-2, we synthesized the 26-amino acid peptide within LRR5 of PLAP-1/asporin. The peptide which was randomly scrambled from the alignment of LRR5/PLAP-1/asporin was used as control (Fig. 4A). LRR5/PLAP-1/asporin at concentrations ranging from 0.1 μM to 10 μM showed inhibitory effects on BMP-2-induced ALPase activity and osterix mRNA expression (Fig. 4B and C). When we also stimulated MPDL22 cells with BMP-2 in the presence of LRR5/PLAP-1/asporin, the phosphorylation of Smad1/5/8 was inhibited (Fig. 4D) as was found with full length recombinant PLAP-1/asporin protein.

Discussion

In this paper, we revealed that PLAP-1/asporin acted as a negative regulator of BMP-2-induced cytodifferentiation of PDL cells *in vitro* by inhibiting BMP-Smads signal transduction via the center part of the LRR domain of PLAP-1/asporin.

Recombinant PLAP-1/asporin protein showed a BMP-2 inhibitory effect in PDL cells. This result was consistent with our previous finding that PLAP-1/asporin-overexpressing cells showed hyporesponsiveness to BMP-2. However the inhibitory effect of PLAP-1/asporin was not dose-dependent as was the case with the LRR5/PLAP-1/asporin peptide. This may be at least partially explained by the phenomenon that the expression of endogenous PLAP-1/asporin mRNA was significantly suppressed by adding of 1 μg/ml of PLAP-1/asporin (data not shown). Moreover, we previously reported that the expression of PLAP-1/asporin was induced by BMP-2 [19]. These facts indicate that PLAP-1/asporin and BMP-2 form a regulatory feedback loop. In Fig. 2B, Smad1 showed the tendency to decrease slightly as to correlate with its phosphorylation. However, this correlation did not necessarily occur and was not reproducible as seen in Fig. 4D. With the present date, we consider that the phosphorylation of Smad1 may not correlate with its degradation.

Having clarified that PLAP-1/asporin directly binds to BMP-2, we then tried to identify the site(s) which would be involved in the molecular interaction. It has been proposed that decorin binds to TGF-β and collagen through LRR3-5 [11] or LRR4-5 [12]. In addition, peptides derived from human decorin LRR5 have been reported to inhibit angiogenesis [20]. We found in this study that LRR5/PLAP-1/asporin exerted biological activity in inhibiting BMP-2-induced cytodifferentiation. LRR5/decorin was reported to have the same secondary structure as LRR5 of mature decorin. As PLAP-1/asporin shows high conservation of residues compared to decorin, LRR5/PLAP-1/asporin may also have structural effects.

We built a 3D-structural model of mouse PLAP-1/asporin and found ionic residues at the center of the concave surface which might be involved in the PLAP-1/asporin–BMP-2 interaction.